火山 第58巻 (2013)
第2号, CD-BOOK

2013 IAVCEI Field Trip Guide

B02: Active Volcano in Central Japan: Asama Volcano

Maya YASUI*, Masaki TAKAHASHI*, Takashi TSUTSUMI **, Shigeo ARAMAKI***, Minoru TAKEO**** and Yosuke AOKI****

*: *Department of Geosystem Science, Nihon University, Tokyo, Japan*
**: *Asama Jomon Museum, Nagano, Japan*
***: *Yamanashi Institute of Environmental Sciences, Yamanashi, Japan*
****: *Earthquake Research Institute, University of Tokyo, Tokyo, Japan*

1. Introduction

Asama volcano, located near the Tokyo metropolitan area, is one of the representative active andesitic volcanoes in Japan. It has erupted repeatedly in historical times. The famous large-scale plinian eruption occurred in 1783 A.D. It has had frequent vulcanian eruptions since the beginning of the 20th century, and small eruptions recently occurred in 2004 and 2009 A.D.

The 1783 A.D. eruption ejected airfall pumice, pyroclastic flows, and lava flows. It has been considered as a continuous one-cycle eruption, which began with the ejection of airfall pumice and ended with the effusion of a lava flow. Recent study, however, has revealed that the airfall pumice, pyroclastic flows, and lava flows were erupted nearly contemporaneously and that the lava flows were clastogenic. In this guide and field excursion, we will focus on the eruptive products of 1783 A.D., with an emphasis on their mode of eruption and emplacement.

In this guide, geological setting of Asama volcano is presented in chapter 2. The eruptive history of the volcano, including stratovolcanoes, pyroclastic cones, and lava domes, is explored in chapter 3. The great eruption in 1783 A.D. is treated in chapter 4. First, it provides overview of the eruptive sequence. Next, description of characteristics of the eruptive products and its stratigraphy are presented. Focusing on the 1783 eruption, we will discuss the eruption style based on the latest research on the proximal depositional processes of pyroclastic materials, which form pyroclastic cones and clastogenic lava during a plinian eruption. The archaeological sites destroyed by the 1783 eruption are also described in this chapter. Petrology is summarized in chapter 5. Monitoring of Asama volcano is treated in chapter 6 and magma path way is discussed. Volcanic hazards and mitigation of volcanic disasters are provided in chapter 7. Description of the field trip stops are presented in the last.

2. Location and geologic setting of Asama volcano

Asama volcano is situated about 160km northwest of Tokyo, at the junction of the Northeast Japan and Izu-Mariana arcs (Fig. 1). The front of the Northeast Japan volcanic belt makes a sharp turn near the site of Asama volcano. Because it sits on the volcanic front, Asama volcano is the farthest from the trench, but the chemistry of its volcanic rocks (i.e., low in alkali content) is characteristic of volcanoes that lie along the volcanic front.

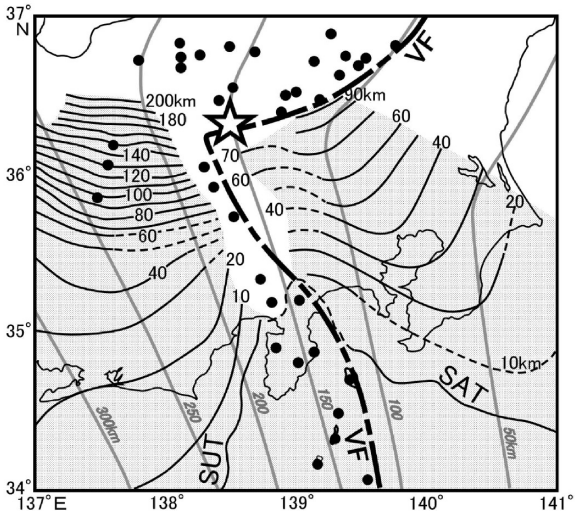

Fig. 1 Map showing the location of the Eboshi-Asama volcano group. The contour lines of depth are subducting plates which are cited from Nakajima and Hasegawa (2007). Open star: Eboshi-Asama volcano group, solid circle: Quaternary volcano, VF: Volcanic front, solid circle: Quaternary volcanoes, SAT: Sagami trough, SUT: Suruga trough, black numerals: the depth of the surface of the subducting Philippine-sea plate in km; gray numerals: the depth of the surface of the subducting Pacific plate in km.

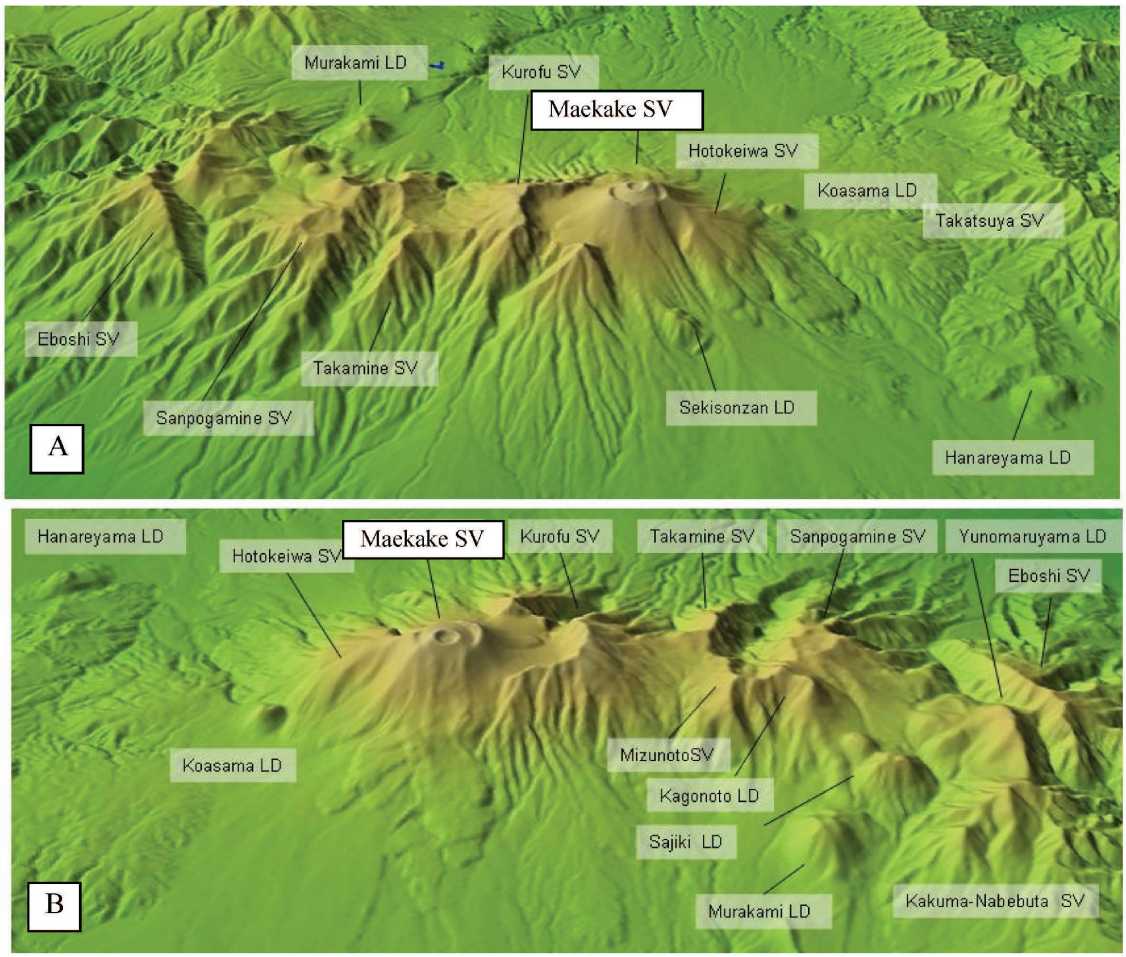

Fig. 2 Bird's-eye view of the Eboshi-Asama volcano group.
A: view from the south, B: view from the north.
SV: stratovolcano, LD: lava dome.

The volcano is located in the center of a large (30km×20km) tectonic depression with a negative gravity anomaly of more than 20mgal. The depression was probably formed within the Neogene volcanogenic formations, which constitute the eastern margin of Fossa Magna, a great rift-like tectonic zone separating northeastern Honshu from southwestern Honshu. Immediate basement rocks are Pliocene (ca. 3Ma) subaerial pyroclastic rocks and welded tuffs (Shiga welded tuff) lying to the south and east of the volcano.

3. Geology and eruptive history of Eboshi-Asama volcano group

3-1. Eboshi-Asama volcano group

To the west of Asama volcano, there is an older Quaternary volcano called the Eboshi volcano group. The volcanism appears to have progressed eastward, with Asama volcano as its eastern end and the youngest member of the row. The row as a whole, including Asama volcano, is called the Eboshi-Asama volcano group, which extends about 22 km from west to east (Fig.2).

The Eboshi volcanic group comprises at least three large stratocones with small stratocones and lava domes. The youngest member of the oldest Eboshi volcano, one of the large stratocones, is 0.37 to 0.35Ma by K-Ar dating (Takahashi and Miyake, 2004). Sanpo stratocone to the east of Eboshi volcano is 0.32 to 0.22Ma (Takahashi *et al*., 2013), and Takamine stratocone to the east of Sanpo volcano is 0.24 to 0.16Ma (Takahashi *et al*., 2013). The large stratocones become younger eastward. Murakami and Kagonoto volcano, one of the lava domes, is 0.08 to 0.07Ma (Takahashi *et al*., 2013). The lava domes aligned from west to east are the youngest in the Eboshi volcano group, and their activities overlapped with the early stage of Asama volcano.

Immediately beneath the edifice of the present-day Asama volcano, strongly dissected older volcanic bodies are probably present. Several Quaternary andesitic volcanoes, older than Asama, extend east of Asama, forming an irregular but generally flat

topography. Takatsuya volcano, one of these older volcanoes, is 0.13Ma (Kaneko *et al.*, 1989). Asama is only one of a group of these Quaternary volcanoes with various sizes and structures, but it is distinct because of its extreme youth.

Asama volcano itself is a complex of three volcanic edifices: Kurofu, Hotokeiwa, and Maekake, each of a different eruptive type (Fig. 3). The oldest, Kurofu volcano, is a large andesitic stratocone; the second oldest, Hotokeiwa volcano, is a medium-sized edifice with rhyolitic to andesitic composition. It is a pile of lava flows with gentle slope. It was accompanied by voluminous pyroclastic flow deposits. Maekake, the youngest volcano in the Eboshi-Asama volcano group, is a medium-sized andesitic pyroclastic cone with pyroclastic flows and lava flows.

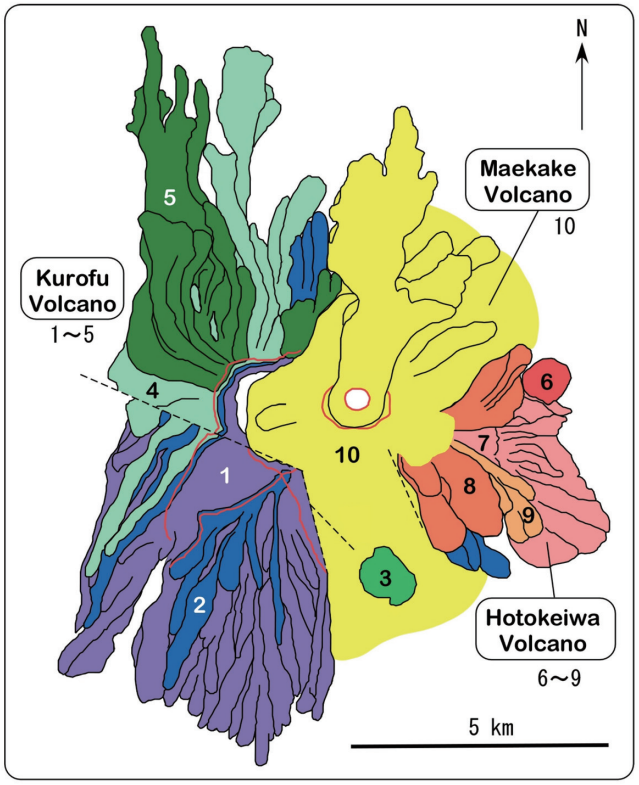

Fig. 3 Geologic map of Asama volcano.
1: Gippa lava group, Kurofu volcano (lava and pyroclasts); 2: Kengamine lava group, Kurofu volcano (lava and pyroclasts); 3: Sekisonzan lava dome; 4: Mitsuone lava group, Kurofu volcano (lava and pyroclasts); 5: Sennin group, Kurofu volcano (lava and pyroclasts); 6: Koasama lava dome; 7: Lower member of Hotokeiwa lava, Hotokeiwa volcano; 8: Middle member of Hotokeiwa lava, Hotokeiwa volcano; 9: Upper member of Hotokeiwa lava, Hotokeiwa volcano; and 10: Maekake volcano. Broken line: fault. Red line: edge of cliff.

3-2. Kurofu volcano

Kurofu volcano is the largest edifice and occupies the western part of Asama volcano (Fig. 4). It was originally a symmetrical stratocone, probably reaching 2,800m above sea level, and is composed of an alternation of andesitic lava flows and pyroclastic materials. The core of the cone is now exposed as pointed peaks on the widened crater wall. A huge landslide, possibly triggered by a plinian eruption (As-BP4) at about 23ka, removed the eastern half of the crater wall and the lower slopes (Takemoto, 1999). The debris avalanche deposits are now found on the southeastern (the Shiozawa deposit), southwestern (the Tsukahara deposit), and northern (the Okuwa deposit) slopes, forming a characteristic hummocky topography. The southwestern sector of the Kurofu cone is breached by a large valley of the Jabori River, which drains the old crater of Kurofu volcano.

The lower two thirds of the Kurofu cone consist of a rather homogeneous alternation of lava flows and tuff breccias produced by strombolian to vulcanian eruptions, which must have grown in a relatively short time period; they comprise the lower Gippa and upper Kengamine lava groups (Fig. 5). The lavas of the Gippa lava group are mafic to intermediate andesite and the least SiO_2-enriched members of the Asama volcano, while those of Kengamine lava group are intermediate andesite and rather SiO_2 rich. After a slight unconformity, the alternation of andesitic lava flows and pyroclastics forms the middle member (the Mitsuone lava group), which is intermediate andesite and was formed by strombolian to vulcanian eruptions. A lava dome of felsic andesite called Sekisonzan, which belongs to the Kengamine lava group, is located on the southern middle flank of Asama volcano.

The lavas of more felsic andesite of the Sennin group overlay the Mitsuone lava group with angular unconformity. The Sennin group consists of felsic andesite and stratified, densely welded, lava-like pyroclastic rocks. The Mitsuone lava group was produced by plinian to sub-plinian eruptions.

The Gippa and Kengamine lava groups are about 0.09 to 0.08 Ma by K-Ar dating. The tephrochronological study reveals that the Mitsuone lava group, characterized by olivine phenocrysts, was active during the time span of 0.07 to 0.03Ma (Takemoto, 1999). The Sennin group is younger than 0.03Ma and is correlated with the Itahana brown pumice (As-BP) in the northern Kanto plain, the age of which is younger than 29ka.

3-3. Hotokeiwa volcano

In the next episode, the appearance of dacite to rhyolite magma with minor amounts of andesite resulted in voluminous pumice eruptions and the formation of a pile of thick lava flows (Hotokeiwa volcano).

At about 20 to 19ka (Nakamura *et al.*, 1997), a new vent opened about 12km southeast of that of Kurofu volcano, from which a thick lava flow of hornblende-bearing pyroxene dacite, a pumice flow (the Kumoba pumice flow), and a lava dome consisting of quartz-bearing hornblende biotite dacite to rhyolite (the Hanareyama lava dome) were erupted (Fig. 4).

At about 19ka, another vent opened at the present site of a separate hill of Koasama, about 5km east of the Kurofu vent, and produced a pyroxene rhyolitic lava dome with a height of 200m. It was preceded by a heavy ejection of hornblende-bearing pyroxene rhyolitic pumice, which formed a plinian deposit (the Shiraito pumice fall: As-SP) extending to the east. The lower member of the Hotokeiwa lava flow consisting of hornblende-bearing pyroxene rhyolite was probably erupted at nearly the same time from a vent of the Hotokeiwa volcano about 2km east of the Kurofu volcanic center.

Next, at about 17 to 16ka, the first Okubozawa pumice fall (As-OkP1) and the first Okubozawa pumice flow were erupted, followed by the second Okubozawa pumice fall (As-OkP2) and the second Okubozawa pumice flow of similar composition and erupted from the same vent.

The Itahana yellow pumice fall (As-YP), first Komoro pumice flow, Tsumagoi pumice flow, and Tsumagoi pumice fall (As-YPk) were erupted in succession at about 14ka (Aramaki, 1993). The first Komoro pumice flow is the largest of the pumice flows, with a volume of about 4km^3. The axis of dispersal of As-YPk extends to the northeast. The middle member of the Hotokeiwa lava flow consisting of pyroxene dacite, which is similar in composition to these pyroclastic deposits, probably poured out in this stage. The pumice flows spread over the northern and southern slopes of Asama volcano, covering an area of more than 200km2. The deposit is mostly not welded, containing abundant pumice lumps, lithic fragments, and charred tree trunks. The thickness exceeds 30m, and many flow units are recognizable due to grain-size differences. The flat plain south of Karuizawa was flooded due to the damming of rivers by the pumice flow.

The final voluminous eruptive products of Hotokeiwa volcano were the second Komoro pumice flow and the Soja airfall pumice at about 11ka (Takemoto, 1999). The upper member of the Hotokeiwa lava flow composed of silicic pyroxene andesite was effused by this eruption.

The edifice of Hotokeiwa volcano, a flat shield of lava about 400m thick, was thus formed probably between 19 and 11ka.

The eruption of voluminous pumice flows and falls triggered a collapse around the vent area. Although the precise outline of the depression is not known, the collapse formed a graben-like structure about 2km wide trending north-south, crossing the center of eruption of Hotokeiwa volcano. The lava shield was broken by faulting, and its western and northern sectors are now completely lost.

Fig. 4 Asama volcano seen from the southeast. The Hanareyama lava dome and Karuizawa town, a popular international resort, can be seen in the foreground.

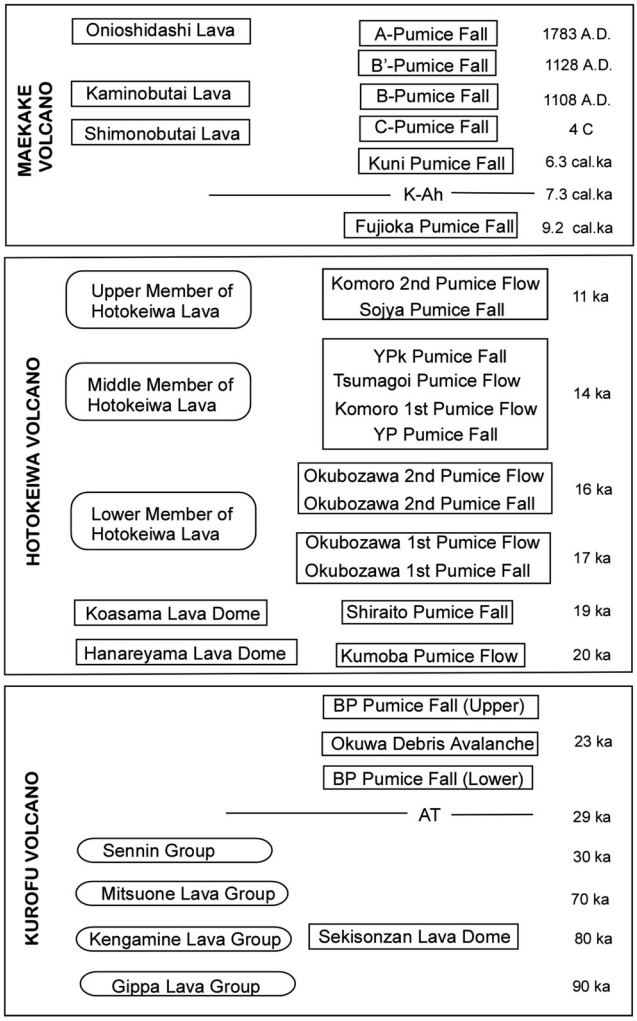

Fig. 5 Eruptive history of Asama volcano.

3-4. Maekake volcano

A new volcano, Maekake, began to grow over this complex heap of broken volcanic edifices (Fig. 6). Its vent is located close to that of Hotokeiwa volcano, and as the new stratovolcano grew, it buried the graben and almost completely covered the topographic irregularities of the pre-Maekake edifices. The new volcano consists of an alternation of porphyritic andesite lava flows and pyroclastics, now reaching an altitude of 2,560m. Thus, the Maekake volcano comprises only a minor portion of the whole Asama volcano, but it overlies and conceals the complex structure of older members.

The construction of Maekake volcano began in 13cal.ka (11ka), just after the cessation of the activity of Hotokeiwa volcano. The eruptive history of Maekake volcano consists of two contrasting stages: active and dormant. The active stage comprises both plinian (including sub-plinian) and vulcanian (including strombolian) eruptions, with the former being large-scale and the latter ranging from intermediate to small-scale.

The first dormant stage, covering the time span from 13 to 9.2cal.ka, continued for about 3,800 years and accompanied several large vulcanian eruptions. The first active stage, with a duration of about 600 years, comprised the two plinian eruptions: the Fujioka pumice fall deposit (Fo) in 9.2cal.ka (ca.0.19km^3 DRE) and the Kumakawa pumice fall deposit in 8.6cal.ka (ca.0.07km^3).

The second dormant stage commenced in 8.6cal.ka and continued to 6.3cal.ka, a duration of about 2,300 years, during which the two large vulcanian eruptions occurred. The second active stage, which lasted for about 1,100 years, consisted of the four plinian eruptions, which gave rise to the Kuni pumice fall deposit (Kn) in 6.3cal.ka (ca.0.29km^3), the Miyota pumice fall deposit (My) in 6.1cal.ka (ca.0.13km^3), the Sengataki pumice fall deposit (Se) in 5.7cal.ka (ca.0.04km^3), and the D pumice fall deposit (D) in 5.2cal.ka (ca. 0.13km^3).

The third dormant stage, with a time span from 5.2cal.ka to the fourth century, continued for about 3,600 years, during which three ashfall deposits were produced by large vulcanian eruptions. The third active stage, with a duration of at least about 1,650 years, included the historical eruptions, namely, the plinian eruptions in the fourth century (ca.0.5km3), 1108 A.D. (ca.0.95km^3), 1128 A.D. (As-B') (ca.0.02km^3), and 1783 A.D. (ca.0.57km^3). The eruptive volume of the large-scale eruption in the third active stage was larger than those in the previous stages (Fig. 7).

The periods in the active stage between the plinian eruptions further consisted of two substages: continuously eruptive and relatively quiescent (Fig. 8).

Maekake volcano is not a typical stratovolcano composed of lavas and pyroclastic rocks but a densely welded pyroclastic cone. The plinian eruption was not a typical one-cycle eruption in which the pyroclastic fall, pyroclastic flow, and lava flow were ejected in this order; instead, the eruptions of pyroclastic fall, pyroclastic flow, and clastogenic lava overlapped. The volcanic cone of Maekake volcano has grown with every plinian eruption, especially the historical large-scale eruptions, which contributed to the construction of the essential portion of the present volcanic edifice. The vulcanian eruptions did not play an important role in the formation of the volcanic cone.

Since the 1783 eruption, thousands of small-scale vulcanian explosions at the summit crater have been recorded (Fig. 9). The repose intervals of the explosions varied from less than a day to several tens of years. The explosions were frequent from 1927 to 1961 (up to several hundred times per year) but have been rare since 1982. Intermittent vulcanian explosions, including a strombolian eruption, occurred in 2004 and lasted for about two months. New lava appeared at the crater bottom. The last small-scale explosion occurred in 2009. Each explosion ejected bombs and blocks (in the order of 104 tons or less) near the crater and rarely deposited ash and lapilli onto the distal parts of the volcano (e.g., Minakami, 1942a; Aramaki and Hayakawa, 1982).

(written by M. Takahashi)

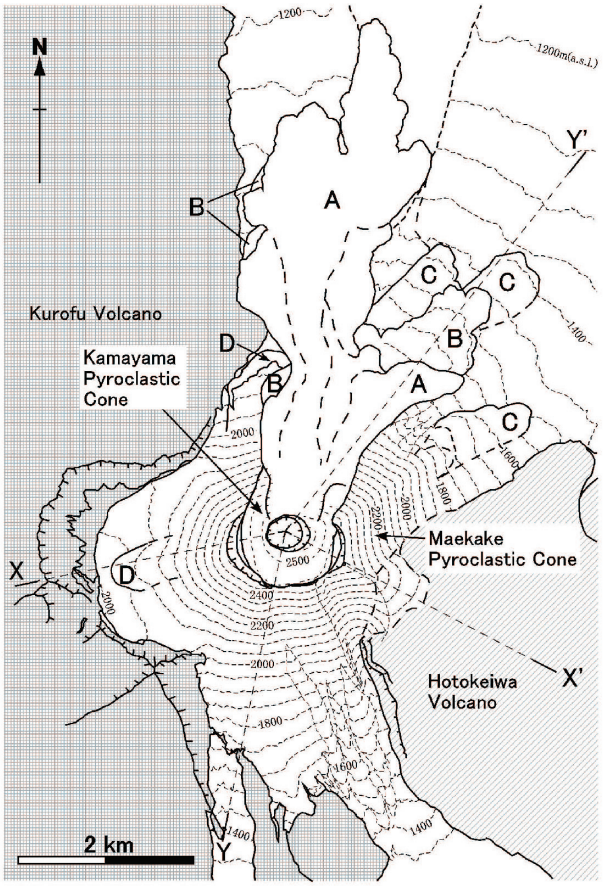

Fig. 6 Geological sketch map of the Asama-Maekake volcano (Takahashi *et al.*, in preparation). A: Onioshidashi lava (1783 A.D.), B: Kaminobutai lava (1108 A.D.), C: Shimonobutai and Kuromamegawara lava (4th century), D: Lavas erupted in 5.2cal.ka.

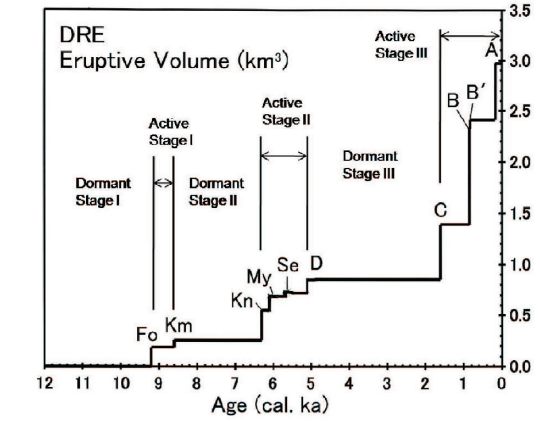

Fig. 7 Diagram showing the relationship between eruptive volume (km^3) and age of eruption (cal.ka) (Takahashi *et al.*, in preparation). Fo: Eruption of Fujioka pumice, Km: Eruption of Kumakawa pumice, Kn: Eruption of Kuni pumice, My: Eruption of Miyota pumice, Se: Eruption of Sengataki pumice, D: Eruption of5.2cal.ka, C: Eruption of 4C, B: Ten-nin eruption (1108A.D.), B': Daiji eruption (1128A.D.), A: Tenmei eruption (1783 A.D.)

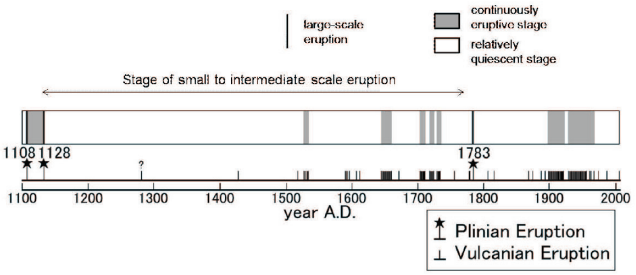

Fig. 8 Diagram showing the eruptive events of Maekake volcano since the large-scale eruption in 1108 A.D. (Takahashi *et al.*, in preparation).

Fig. 9 Summit crater of Kamayama seen from the NE. Repeated vulcanian eruptions have occurred at this crater after the 1783 eruption.

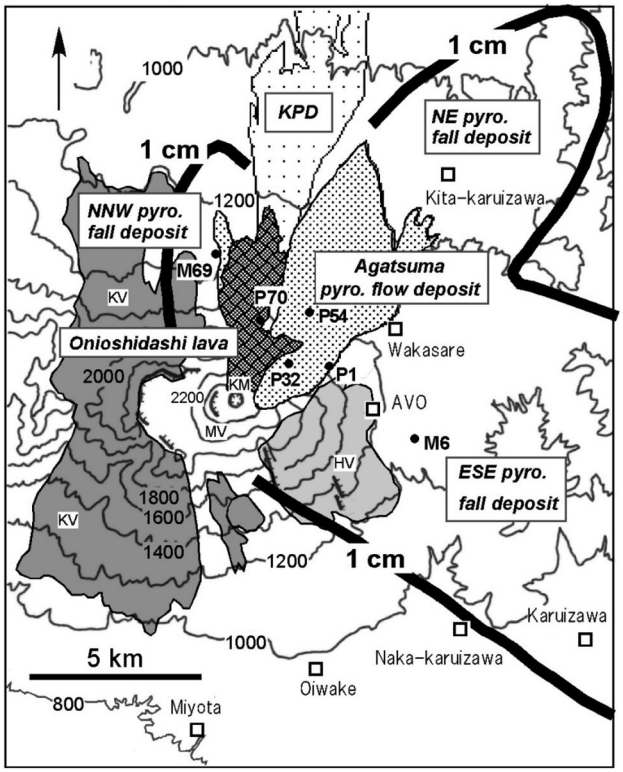

Fig. 10 Map showing the distribution of the 1783 eruptive products and a simplified geological map of Asama volcano after Aramaki (1963), showing the three major volcanic edifices (Kurofu, Hotokeiwa, and Maekake volcanoes). P1, P32, P54, P70, M6, and M69 are the localities described in the text and in Fig. 12. The stops in the field trip are also shown on the map. KPD: Kambara pyroclastic flow / debris avalanche deposit, AVO: Asama Volcano Observatory, University of Tokyo.

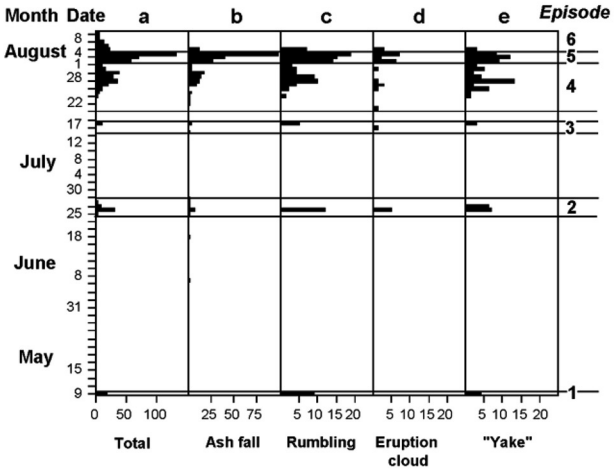

Fig. 11 Frequency diagram showing the number of descriptions in the old documents (Yasui and Koyaguchi, 2004).
a: Total number, b: number of localities where pyroclastic material had fallen, c: number of localities where rumbling was audible, d: witnessed eruptive column and/or eruption cloud, e: number of descriptions of *yake*, which means the occurrence of an eruption, rumbling, an eruptive column, and/or an eruption cloud in a more general sense.

4. The great eruption in 1783 A.D.

4-1. Sequence of the 1783 eruption

The 1783 eruption (Tenmei era) is the latest large-scale explosive eruption of Asama volcano. Many previous studies of the eruption have been reported (e.g., Minakami, 1942b; Aramaki, 1956, 1957). Yasui and Koyaguchi (2004) discussed the eruptive style based on the geology and old documents. Figure 10 shows the distribution of the 1783 eruptive products. The total volume of the eruptive products is estimated to be about 0.5km^3. The three-month eruption, which started on 9th May, is divided into six episodes on the basis of the waxing and waning inferred from old records made during the time of eruption (Fig. 11). For the definition of the terms “episode” and “phase,” see the caption in Fig. 13.

The intervals between the episodes became shorter over time. Episodes 1 to 4 were intermittent vulcanian or plinian eruptions, which generated several pumice fall deposits. Episode 5 is subdivided into many eruptive phases. During Episode 5, the duration of individual eruptive phases and the mass of the erupted magma increased exponentially. The intensity of the eruption increased dramatically in Episode 5, which started on 2 August, and culminated in a final phase that began on the night of 4 August and lasted for about 17 hours. This climactic phase is further divided into two subphases (Fig. 13). The first subphase is characterized by the generation of a pumice fall, while the second one is characterized by abundant pyroclastic flows. The stratigraphic relationships suggest that the rapid growth of a cone and the generation of clastogenic lava flows occurred simultaneously with the generation of pumice falls and pyroclastic flows. The details are mentioned in section 4-2. The climactic eruption ceased early in the morning of 5 August 1783. After an interval of several hours, a series of peculiar events occurred as Episode 6. At 10 a.m. on 5 August, a large explosion with a loud booming sound occurred, and a pyroclastic flow and debris avalanche was generated, which moved toward the northern foot of the volcano, devastating a village on its way (Aramaki, 1956). The avalanche then entered

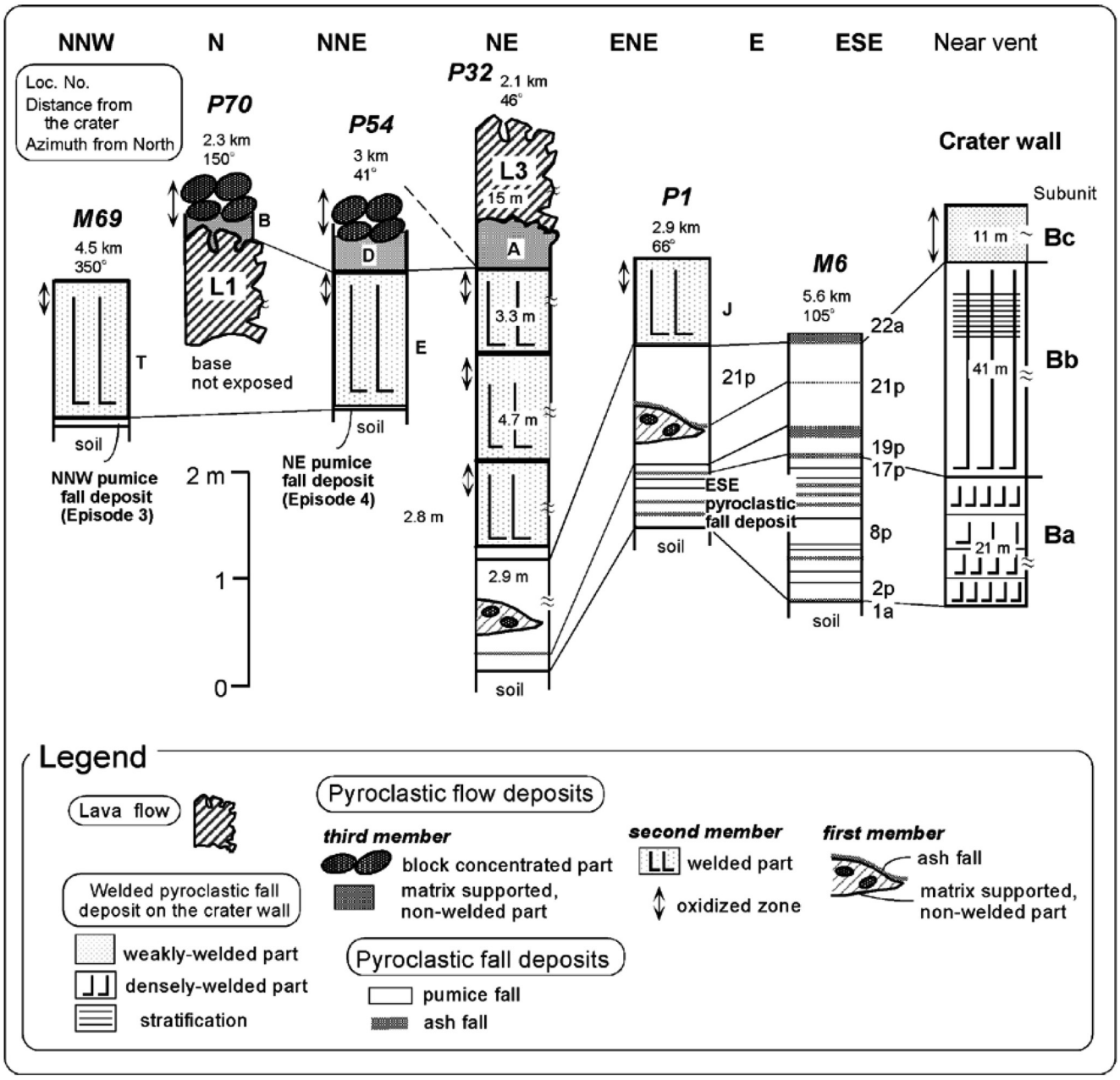

Fig. 12 Representative columnar sections showing the stratigraphic relationships between deposits extending in different directions (Yasui and Koyaguchi, 2004). The localities are shown in Fig. 10.

the Agatsuma River, transforming it into a water-saturated mudflow and water flood. The mudflow and flood caused a disaster, killing more than 1500 people even in the distal areas up to several hundred kilometers from the volcano.

4-2. Geological features and eruptive style of the 1783 eruption

The 1783 eruptive products are distributed widely around the volcano (Fig. 10). Figure 12 shows representative columnar sections of the deposits and the stratigraphic correlations. The eruptive sequence was reconstructed based on the stratigraphy described below.

Pyroclastic fall deposits

The main part of the 1783 pyroclastic fall deposits extends toward the ESE, while thin (up to 13 cm) pale-gray pumice fall layers are found to the NNW and NE (Figs. 10 and 14). Because there is a good correlation between the distribution of the deposits and the area of ashfall recorded in the old documents, a detailed time axis can be given to the stratigraphy (Yasui *et al*., 1997). The NNW and NE pyroclastic fall deposits were most likely deposited during Episodes 3 and 4, respectively. The ESE pyroclastic fall deposits consist of a lower, stratified part with many pumice fall layers and an upper, thick pumice fall layer. It is made up of twenty-two fall units of pumice and ash. Figure 12-M6 shows a representative stratigraphic section of the ESE fall deposits (Loc.M6: 5.6 km, E15°S from the summit crater). The upper half (Layer 21p) is composed of a single massive layer, although it rarely shows weak stratification. Layer 21p is the thickest and coarsest-grained. Most of the ESE pyroclastic fall deposits correspond to Episode 5, whereas the lowermost part corresponds to Episode 4. The upper half of the ESE pyroclastic fall deposits corresponds to the first subphase of the final phase of Episode 5, which was the climactic eruption of the 1783 sequence. Therefore, this indicates that the pumice fall deposits of the lower half of the ESE deposits (up to Layer 19p) were originated from the intermittent eruptions, after which the upper, coarse, thick pumice fall layer (Layer 21p) was generated by the climactic plinian eruption in the final phase of Episode 5.

The ESE pyroclastic fall deposits contain several fine-ashfall layers: 1a, 5a, 10a, 12a, 14a, 18a, 20a, and 22a (Fig. 12-M6). These ash layers, except for Layer 1a, consist of glass shards, crystal debris, and small amounts of lithic fragments and show various colors, including pinkish gray, light brown, and light purple. Each ash layer tends to thicken toward the area where the pyroclastic flow deposits are concentrated (i.e., the ENE flank of the volcano) rather than toward the vent. One of the fine-ashfall layers can be traced to an ash layer that directly covers the pyroclastic flow deposits (see P1 and M6 in Fig. 12). This suggests that at least some of the ashfall layers were derived from the ash clouds of pyroclastic flows. Because many ash layers are intercalated with the lower half of the ESE pyroclastic fall deposit, small-scale plinian eruptions and generation of pyroclastic flows are believed to have occurred repeatedly before the climactic plinian eruption.

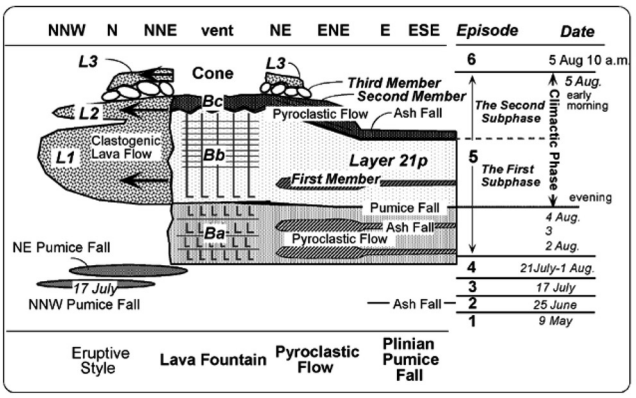

Fig. 13 Schematic illustration of the eruptive sequence of the 1783 eruption (Yasui and Koyaguchi, 2004). The term "episode" is used here to refer to an active period, which is inferred from the change in the number of descriptions in the old documents (Fig. 11). One episode is separated from another by a distinguishable repose period of more than a few days or a period of markedly weaker eruptions. The individual episodes are composed of single and/or multiple "phases." The term "phase" is used to refer to a single eruptive event in the old documents. When one phase can be further divided into subgroups for a certain reason, such as a change in eruptive style, we use the term "subphases." Generally, an individual phase or subphase includes explosions or other fluctuations in the magma discharge rate over a time frame of several to a few tens of minutes.

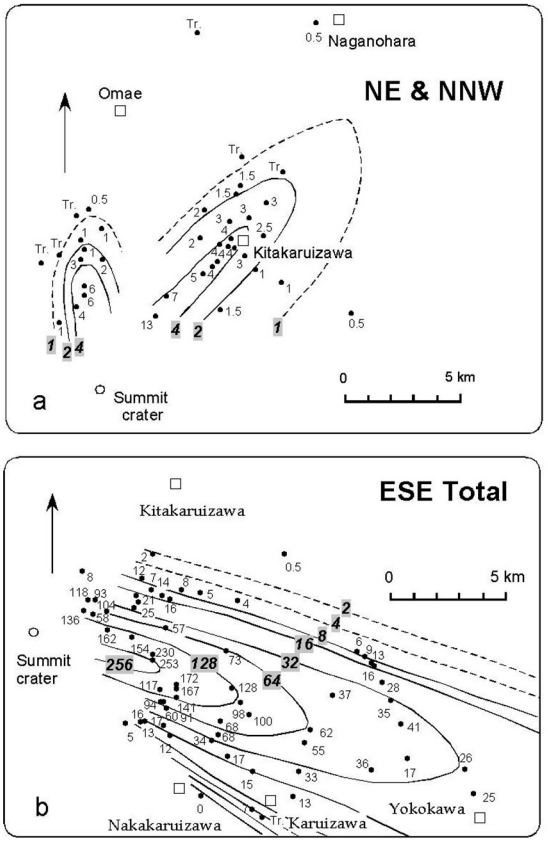

Fig. 14 Isopach map of the 1783 pyroclastic fall deposits in cm (modified from Yasui *et al*, 1997). a: NE and NNW pyroclastic fall deposit, b: ESE pyroclastic fall deposit (total).

Pyroclastic cone

The edifice named Kama-yama is a pyroclastic cone on the summit of Asama volcano. It occupies a saucer-like, shallow depression on the somma, Maekake-yama, and rises from the northern slope of Maekake-yama (Fig. 15). The altitude of the summit of Kama-yama (2568 m) is higher than that of Maekake-yama (2524 m). According to old documents, Maekake-yama was higher than Kama-yama before the 1783 eruption. Old drawings described the rapid growth of the cone during the eruption. These records, as well as the following geological evidence, suggest that Kama-yama formed during the 1783 eruption (Yasui and Koyaguchi, 1998). A stratified section of the cone (>100 m thick) is exposed on the inner crater wall (Fig. 9). The crater wall sequence is divided into three parts based on the unconformities and differences in lithology: Units A, B, and C in ascending order (Fig. 16). These units are deposits of pyroclastic fall or lava fountains, judging from the fact that these layers mantle underlying topographic undulations with uniform thickness. Units A and B are alternations of welded and non-welded pyroclastic deposits, and they are separated from each other by a distinct erosion surface. Unit C consists of recent vulcanian deposits. Unit B is stratigraphically correlative with the deposits of the 1783 eruption (Yasui and Koyaguchi, 1998). This interpretation is consistent with the fact that the altitude of the bottom of Unit B is lower than the altitude of Maekake-yama.

Unit B is further subdivided into three subunits: Ba, Bb, and Bc (Fig. 16). Subunit Ba is composed of several cooling-units of pyroclastic fall. Each cooling unit, recognized by columnar joints of a distinct width, is several meters in thickness. Subunit Bb is a massive, densely welded pyroclastic fall deposit. Although it shows a weak stratification in the upper part, Subunit Bb has wide columnar joints crossing through its whole thickness, indicating that the subunit consists of a single cooling unit. Subunit Bc is composed of weakly welded, stratified layers of oxidized pyroclasts.

Both the sequences of Unit B and the ESE pyroclastic fall deposits are characterized by a stratified lower half and a massive upper half. This pattern is consistent with the fact that the eruption started with intermittent explosions, followed by a continuous, plinian eruption in the climactic phase. It has been suggested that the cone formation and plinian eruptions occurred simultaneously and that Subunit Bb may be correlative with the plinian deposits of the climactic phase (Layer 21p). This is consistent with several old drawings (e.g., Fig. 23) showing abundant incandescent spatter falling onto the vent area coeval with a plinian eruption column, suggesting that contemporaneous fountains formed a cone around the vent during the plinian eruption.

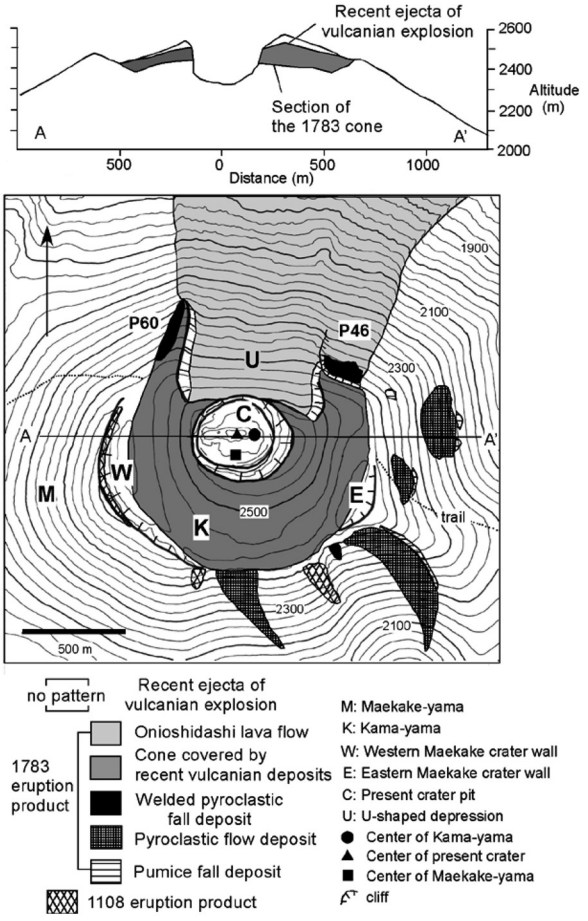

Fig. 15 Map showing the topography and geology around the summit region of Asama volcano (Yasui and Koyaguchi, 1998). The values in the contours show the altitude in meters. P46 and P60 are well-exposed outcrops of agglutinate. The east-west cross section (A-A') is also shown.

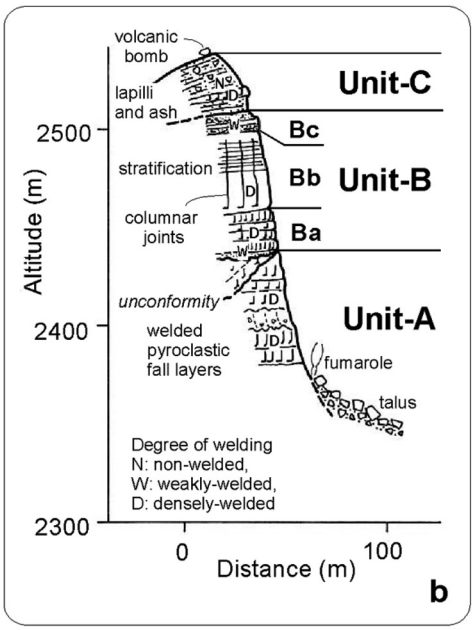

Fig. 16 Schematic columnar section of the crater wall of Kamayama (Yasui and Koyaguchi, 1998).

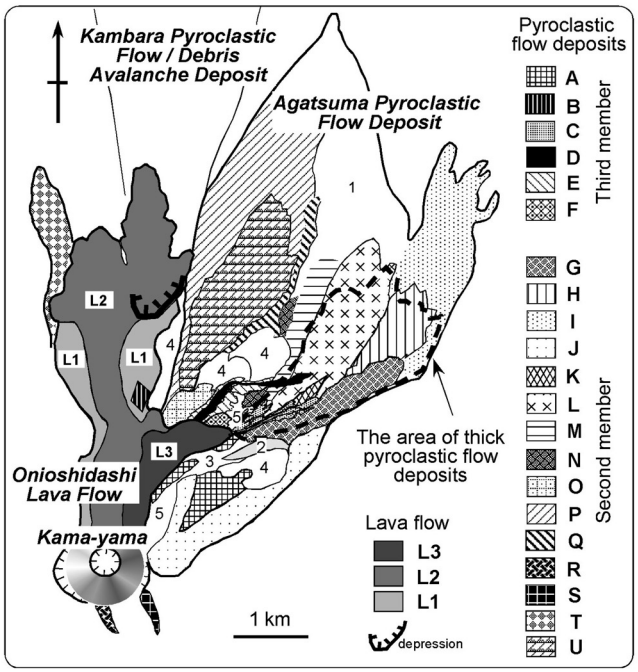

Fig. 17 Map showing the distribution of units of the 1783 pyroclastic flow deposits (Units A to U) and lava flow (Onioshidashi lava) (Yasui and Koyaguchi, 2004). L1-L3 show the units of the lava flow defined by Inoue (1998). 1: Distal part of the 1783 pyroclastic flow deposits, where the boundaries of the flow units are not well-defined; 2: The first member of the 1783 pyroclastic flow deposit, which is interbedded with Layer 21p; 3: Secondary deposits derived from the 1783 pyroclastic flow deposits of the upper stream; 4: Area where the 1783 pyroclastic fall deposits overlie the pre-1783 eruptive products; 5: The ejecta of the 1108 A.D. eruption. The 1783 pyroclastic flow deposits are thickest in the area enclosed by a dashed line.

Lava flows

The lava flows of the 1783 eruption are grouped together as the Onioshidashi lava flow (Aramaki, 1956). These lava flows have the surface morphology as typical "block lava," and a lava levee, lateral cliff, and terminal cliff are well developed. Three flow units are recognized, denoted as L1, L2, and L3 in the order of generation (Inoue, 1998) (Fig. 17). L1 and L2 are the main flows extending to the north, while L3 forms a branch to the northeast. L1 and L2 can be traced to the northern, shallow depression on the outer slope of the cone just below the summit crater (Figs. 15 and 17). L3 can be traced not to the crater but instead to a collapsed depression on the northeastern outer slope of the cone, suggesting that it is a rootless flow that originated during a partial collapse of the outer slope of the cone.

The lava flows have unique surface and internal structures. The uppermost 10 m is composed of welded pyroclastic materials (Inoue, 1998). The degree of welding tends to increase downward to a given locality. The non-welded parts consist of oxidized, reddish-brown scoria. In the densely welded parts, macroscopic and microscopic reddish-brown fiamme (the so-called eutaxitic texture) are extensively observed. Also, the content of broken crystals is characteristically high (more than 80%) in all localities.

The internal structure of the lava flow can be observed from a 64m-thick borehole core drilled in the downstream section. The upper half of the core consists of porous, reddish-brown, strongly oxidized materials, while the lower half consists mostly of massive light-gray lava. Eutaxitic textures with pinkish-gray, gray, and dark-gray lenses are common in the densely welded parts (Fig. 18). Abundant broken crystals are contained in the lava throughout the section. These surface and internal structures suggest that the lava flows were originally formed by pyroclastic materials rather than erupted as coherent lava (i.e., clastogenic lava flow).

The lava directly continues upward to the Kamayama pyroclastic cone (Fig. 19). The center of Kamayama is located about 150m NE of Maekakeyama. Thus, the northern part of the cone rises out on the steep outer slope of Maekakeyama (Fig. 15). There is a U-shaped, shallow depression on the northern part of the cone. However, the partial collapse of the cone does not explain the generation of the lava because the volume of the collapsed cone is quite small compared with the total volume of lava.

The depression on the northern crater wall does not contain lava, indicating that no lava overflowed after the partial collapse of the cone. Therefore, Unit B on the northern crater wall is considered to correspond to a section of the lava. The lava generation is believed to have occurred simultaneously with the cone growth during the plinian eruption.

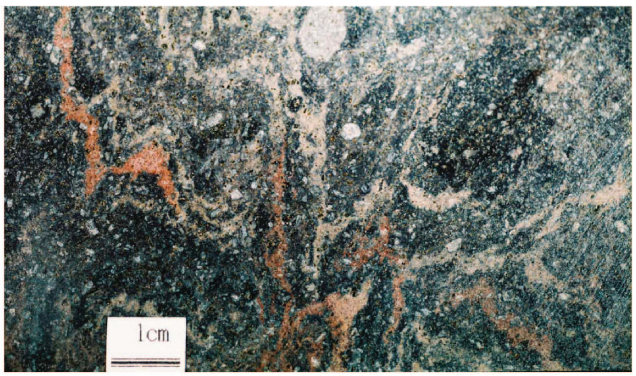

Fig. 18 Photo showing the clastogenic features of the Onioshidashi lava flow and the macroscopic eutaxitic texture in the borehole core sample (depth of 38m).

Fig. 19 Asama volcano seen from the northern sky. Note the summit crater and the lava flow of the 1783 eruption on the northern slope of Maekake volcano.

.

Pyroclastic flow deposits

The 1783 pyroclastic flow deposits, known as the Agatsuma pyroclastic flow, are widely distributed to the northeast, up to 8 km from the summit crater (Fig. 17). Many flow units can be defined on the basis of a vertical change in grain-size distribution, the lithological features of constituent blocks, and the topography. The 1783 pyroclastic flow deposits are divided into three members (Fig. 12). The stratigraphic level of the first member indicates that this member was associated with the climactic plinian eruption in Episode 5 (first subphase). The levels for the second and third members show that these members were generated simultaneously with the later lava (second subphase). The generation mechanism of these pyroclastic flows is still a subject of discussion. Judging from the stratigraphic relations in the ENE flank and the eastern slope, most of the pyroclastic flows are considered to have occurred after the climactic plinian eruption that generated Layer 21p.

In terms of features, the first member is interbedded with Layer 21p. The second member consists the major part of the pyroclastic flow deposits. Although little information is available in the medial area because of poor exposure, the maximum thickness of the second member is estimated to be 40m based on geophysical surveys using an air gun (Shimozuru, 1981). Individual flow units consist of dark-brown scoriaceous blocks and matrix ash. The deposits of the second member are characterized by strong welding. An oxidized zone up to 30 cm thick has developed on the upper surface of some welded layers. The thickness of individual welded layers varies from 3m in the valley to 30 cm toward the ridge. Blocks are not flattened even in the strongly welded part. The presence of thin welded layers and undeformed blocks in the welded layer may indicate that these deposits were emplaced at high temperatures; thus, welding occurred due to sintering rather than compaction. Typically, a vertical variation in degree of welding, an upper oxidized zone, and a thoroughgoing development of columnar joints characterize the second member. The megascopic variation seen in the lithological units reflects various patterns that are useful for establishing the timing of the deposition of different flow units. For example, the fact that different units (or different members) are cut by common cooling joints suggests that pyroclastic flows were generated one after another within a short period of time.

The third member is characterized by strongly developed reverse grading; it consists of an upper clast-supported block-rich zone and a lower matrix-supported zone.

4-3. Syn-plinian vigorous lava fountaining in the climactic eruption

Most magmatic products were generated in the final phase of Episode 5, which was the climax of the 1783 eruption. The lava flows in this eruption characteristically possess abundant broken phenocrysts (more than 80%) and show extensive

"welding" textures. These features indicate that the lava did not effuse as a continuous liquid directly from the crater but as a fountain-fed clastogenic lava. Because the lava flow can be traced directly upward to the crater wall, the cone building and the generation of the clastogenic lava are believed to have progressed simultaneously. The center of the cone is located near the northern edge of the crater rim of the preexisting composite cone, and most of the pyroclasts from the lava fountains are considered to have been deposited on the steep outer slope (up to 30 degrees) of the preexisting cone. The steep slope would promote the continuous flow of the agglutinate. A high magma discharge rate of the lava flow, indicated by its large width, may also suggest that the lava was explosively erupted as a dispersed flow through a conduit rather than as a viscous flow.

Based on the stratigraphic correlation between Unit B on the crater wall and the climactic pumice fall (Layer 21p), a considerable growth and generation of lava is believed to have occurred during the climactic plinian eruption. Therefore, the 1783 eruption shows the features of the formation of proximal cones and the generation of clastogenic flows, as well as the dispersal of the pumice fall in the distal areas (Fig. 20). Concerning the climactic eruption, the volume of pyroclastic materials that fell onto the proximal area is estimated to be 20 times as large as that entrained in the plinian column (Yasui and Koyaguchi, 2004). This indicates that these eruptions have similar aspects to the high fountaining with minor tephra observed at Kilauea and Etna. The coexistence of a plinian column and a lava fountain indicates a complex behavior of erupting magma in the conduit. An annular misty flow in the conduit may be a possible explanation in the case of the 1783 eruption of Asama volcano. That is, a plinian column may originate from a gas-rich center surrounded by a pyroclast-rich lining.

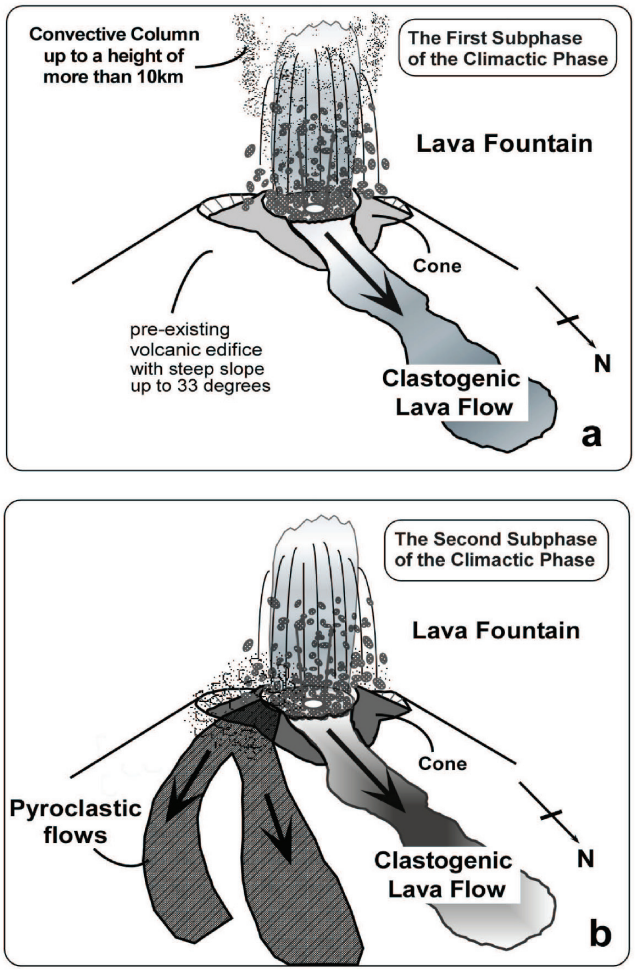

Fig. 20 Schematic illustration of the eruptive sequence of the 1783 eruption. See text for details (modified from Yasui and Koyaguchi, 2004).

4-4. Feature and origin of the Kambara pyroclastic flow/debris avalanche deposit

A mysterious phenomenon (Episode 6 in Fig.13) occurred immediately after the climactic pyroclastic eruption in Episode 5. According to old documents, a loud detonation was heard more than 300 km away at 10 o'clock in the morning of August 5. A devastating flow, which is characterized by containing gigantic essential blocks up to 65 meters in diameter, rushed on the northern foot of the volcano and four villages including Kambara were immediately wiped out by the flow. The flow reached gorge of the Agatsuma River to generate a great flood (Tenmei mud flow) causing a serious disaster (Fig.22). This will be described in detail in the section 4-5-3.

Aramaki (1956) made a detailed description of the deposit on the northern foot of the volcano and revealed that the deposit on the upper stream has nature of pyroclastic flow whereas that on the lower

stream has nature particular to debris avalanche deposit. Therefore, the deposit is called “Kambara pyroclastic flow / debris avalanche deposit” here (KPD hereafter).

There is a depression on the northern flank of the volcano and the KPD distributes north of the depression (Fig.17). Large angular blocks are recognized on the distribution area of the KPD. These blocks concentrate on the upper stream and the number of the blocks decreases downward. Most blocks are essential fragments with characteristic expansion cracks. Based on the N.R.M. measurement, Aramaki (1956) showed that the blocks maintained a temperature above 500°C at the time of emplacement. In contrast to the huge blocks, the thickness of the matrix is thin. It is generally less than several meters. The essential particles compose a small fraction of the matrix. It is mostly made up of fragments derived from the older rocks which directly underlie the KPD. The matrix shows heterogeneous occurrence containing soft blocks of ash derived from pumice flow deposit of Hotokeiwa volcano. A ditch 1.1 to 2km wide develops north of the depression. The older rocks are exposed on the scarps of the ditch on both sides. The presence of abundant accessory materials in the matrix of the KPD and the existence of the ditch indicate that the flow accompanied a significant erosion of the old volcanic edifice. Unusual features of the KPD described above indicate that Episode 6 in the course of the 1783 eruption occurred by chance.

There are at least three different hypotheses to explain the origin of the KPD: (1) an explosion at the summit (Aramaki, 1956), (2) a flank eruption (Inoue *et al*., 1994), and (3) a flank collapse and associated secondary explosion of the Onioshidashi lava flow (Tamura and Hayakawa, 1995). In the hypothesis (1), it is considered that huge hot lava blocks were shot up midair and rained over the steep northern flank to form a high-temperature avalanche (Fig. 21). In the hypotheses (2), a marsh, that existed at the depression of the present day, was noticed and a flank eruption at the marsh was assumed. In the hypothesis (3), a partial collapse of the northern flank probably triggered by an earthquake is thought to cause the secondary explosion of the Onioshidashi lava.

The fact that the distribution of the KPD can be traced to the Onioshidashi lava flow and that the angular juvenile blocks show textures of quenched lava (Tanaka *et al*, 2012) might be in favor of the secondary explosion of the Onioshidashi lava flow. Three units of blast deposit were recognized around the depression suggesting that explosion occurred for at least three times (Tanaka *et al* (2012). Onioshidashi lava, essential materials of the KPD, and those of the blast deposit show quite similar features in bulk rock chemical composition, petrography, and density (Tanaka *et al*, 2012). The similarities between these materials would be a constraint on the origin of the KPD. However, the origin of the KPD is still open to question.

(written by M. Yasui)

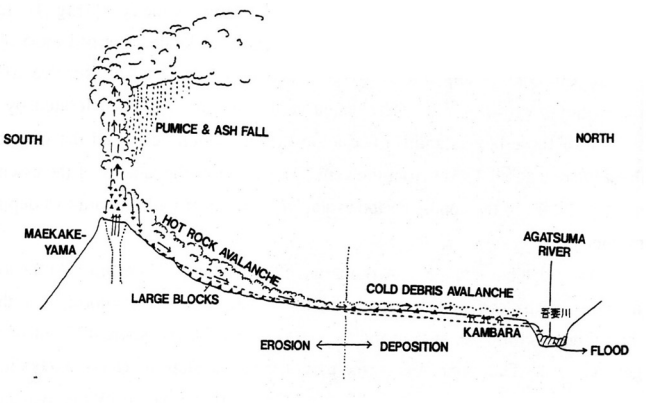

Fig. 21 Schematic diagram showing the mode of emplacement of KPD (Fig.16 in Aramaki and Takahashi, 1992).

4-5. An overview of the archaeological sites destroyed by the 1783 eruption

4-5-1. The archaeological sites destroyed by the 1783 eruption

The 1783 eruption produced pyroclastic flows, lava flows, and a mudflow that covered the northern foothill of Mt. Asama in the Gunma Prefecture (Fig. 22). Pumice fell on the southern foothill of Mt. Asama in the Nagano Prefecture, but no villages were buried under the volcanic products, and therefore no ruins were preserved. The archaeological sites destroyed by the eruption were concentrated in the Gunma Prefecture. In the Nagano Prefecture, where the effects of the eruption were minimal, people made drawings depicting the eruption, and about ten such drawings have been conserved. Because these drawings show that the strongest moment of the 1783 eruption was the plinian eruption (Fig. 23), they are regarded as important documents in the study of volcanology (Asama Jomon Museum, 2004).

The Kambara pyroclastic flow/debris avalanche flowed into Kambara village on the northern foothill of Mt. Asama. When it reached the Agatsuma River, it became the Tenmei mudflow, which destroyed villages along the Agatsuma River.

The Tenmei mudflow also ruined many archaeological sites along the Agatsuma River in the Gunma Prefecture and along the Tone River. Recently, the construction of the Yanba Water Reservoir, a huge water reservoir in the Agatsuma River, led to the excavation of more than 20 archaeological sites along the river. The archaeological records from these excavated sites give us details about the devastated villages and households that were not recorded in historical documents.

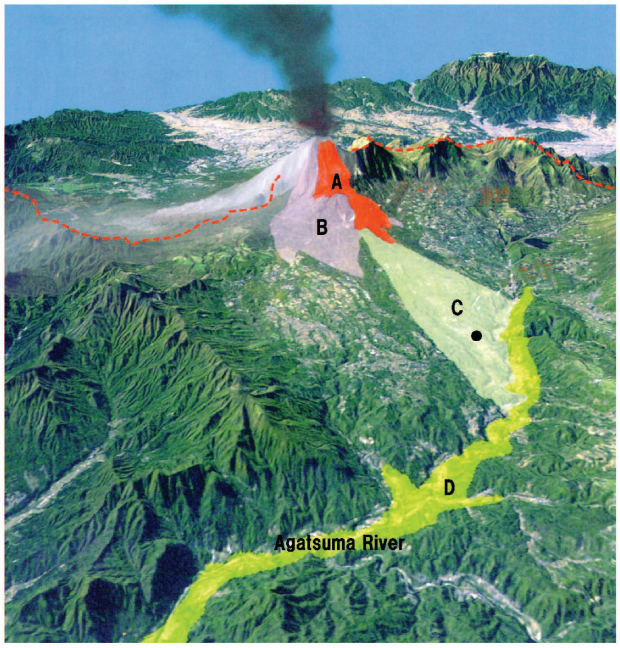

Fig. 22 The 1783 eruptive products that ran down the northern foothill of Mt. Asama (courtesy of the Nagano Prefecture Saku Construction Office). A: lava, B: pyroclastic flow, C: pyroclastic flow/debris avalanche, D: mudflow, ● : Kannondo Temple in Kambara village.

4-5-2. The victims in Kambara village and Kannondo Temple

The most well-known archaeological site destroyed by the 1783 eruption is located under Kannondo Temple in Kambara District, Tsumagoi village, Gunma Prefecture, which is 12 km north of the summit crater (Stop 3-4, Fig. 40); the Kambara pyroclastic flow/debris avalanche buried 35 out of the 50 stone steps of the temple.

In 1979, a team of volcanologists, historians, and archaeologists excavated these buried stone steps. At the lowest step, they found two corpses, the remains of two women who were not able to evacuate in time (Fig. 24). Because no DNA analysis was performed at the time of excavation, the relation between these women, whether they were mother and daughter or mother and daughter-in-law, is not known.

Kambara village, where Kannondo Temple is located, was home to about 570 people living in 100 households. The Kambara pyroclastic flow/debris avalanche killed 466 people, including the two women found in the temple. Ninety-three evacuees survived the eruption. The survivors included those who managed to run up the stone steps, reach beyond the 35th step, and escape from the Kambara pyroclastic flow/debris avalanche, as well as those who were outside the village at the time of the eruption. The products of the eruption killed 170 of the 200 horses in the area. More than 90% of cultivated fields were blanketed by the KPD (Gunma Prefectural Museum of History 1995). As a result of the accumulation of the Kambara pyroclastic flow/debris avalanche, the surface land is more than 5 to 6 m higher today than before the eruption.

4-5-3. The archaeological sites along the Agatsuma River

The estimated number of victims of the Kambara pyroclastic flow/debris avalanche and the Tenmei mudflow is about 1500. Thus, after the debris avalanche had passed over Kambara village, approximately 1000 people were killed along the Agatsuma and Tone Rivers.

The Higashimiya site, which is at the location of the future water reservoir, 20 km away from the summit crater, was excavated starting in 2007; the process took three years to complete. In this site, a residence buried under the Tenmei mudflow, which had accumulated to a thickness of one meter, was recovered from a location 40 m above the bed of the Agatsuma River (Fig. 25). This suggests that the mudflow reached as high as 40 m above the stream at this location. The excavated residence measured approximately 20 by 12 m and was elaborately constructed, with a stable, a bath, and a brewery. It was owned by a rich family that ran a sake brewing factory (Gunma Archaeological Research Foundation, 2011).

The Nakamura site, located on the river terrace along the Tone River, which is about 70 km from the summit crater, was also excavated. The crop field preserved beneath the 4m-thick mudflow yielded domesticated beans. In addition, inkstone, wooden clogs (*geta*), mirrors, chinaware, kettles, and grinding stones were recovered.

The Kamifukushima-nakamachi site, situated 100 km downstream from the summit crater, lies at the edge of the Tone River and yielded eight houses

destroyed by the Tenmei mudflow (Fig. 26). The mud walls of these houses are tilted but not collapsed. This suggests that the intensity of the Tenmei mudflow at this location was not so catastrophic that the mud walls of houses were washed out. The mudflow reached this location more than three hours after its emergence. The historical documents show no record of any victims, suggesting that the intensity of the mudflow had become low enough for people to be able to evacuate to a safe place in time (Seki, 2010).

These archaeological sites, called the *Japanese Pompeii*, preserve evidence of the disaster that took place on the 5th of August 230 years ago. They provide information not only on the lives, culture, and society of people at that time but also on the mechanism of disasters (Tsutsumi, 2012).

(written by T. Tsutsumi)

Fig. 24
The excavated remains of two victims on the stone steps of the Kannondo Temple, which was destroyed in the 1783 eruption (courtesy of the Tsumagoi Village Museum).

Fig. 23 Drawing of the Asama 1783 eruption (courtesy of Mr. Misaizu).

Fig. 25 A residence buried by mudflow at the Higashimiya site (courtesy of the Gunma Archeological Research Foundation).

Fig. 26 The Kamifukushima-nakamachi site: a village along the river that was destroyed by mudflow (courtesy of the Gunma Archeological Research Foundation).

5. Petrology

5-1. Petrography

The rocks of the Gippa and Kengamine groups, the lower and main members of Kurofu volcano, are porphyritic clinopyroxene orthopyroxene andesite to basaltic andesite that are poor in olivine phenocrysts but rich in plagioclase and large clinopyroxene phenocrysts. The Mitsuone group, the middle member of Kurofu, consists of olivine clinopyroxene orthopyroxene andesite characterized by the presence of olivine phenocrysts. The Sen-nin group, the upper member, is composed of clinopyroxene orthopyroxene silicic andesite. The rocks of the Sekisonzan lava dome are also clinopyroxene orthopyroxene andesite.

The lower part of the Hanareyama lava dome is composed of olivine-bearing clinopyroxene orthopyroxene dacite, while the upper part comprises biotite-hornblende-quartz-bearing pyroxene dacite to rhyolite. The rocks of the Koasama lava dome are clinopyroxene orthopyroxene rhyolite. Most lavas of the Hotokeiwa volcano are clinopyroxene orthopyroxene dacite to rhyolite with minor andesite, but some contain phenocrysts of hornblende, quartz, and, rarely, biotite. The essential clasts of the pyroclastic flows and falls of Hotokeiwa volcano are mainly clinopyroxene orthopyroxene dacite to rhyolite and andesite.

The rocks of Maekake volcano are mostly clinopyroxene orthopyroxene andesite with minor olivine phenocrysts.

5-2. Whole-rock chemistry

Kurofu volcano

The volcanic rocks of the Gippa group are poor in SiO_2 content (from 53 to 58 wt% SiO_2, mostly 55 to 56wt%) (Takahashi *et al*., 2008a). The MgO, FeO*, and MnO contents decrease with a slight increase in SiO_2, while Al_2O_3 and Na_2O increase (Fig. 27). The rocks of the Kengamine group range from 56 to 64wt% in SiO_2 content and are richer in MgO compared with those of the Gippa group at similar SiO_2 contents (Takahashi *et al.*, 2008a). The Mitsuone group ranges from 56 to 62 wt% in SiO_2 content, nearly the same as the Kengamine group, but is even richer in MgO (Takahashi *et al.*, 2008a). The Sekisonzan lava dome consists of silicic andesite (63 to 64wt% SiO_2) and has MgO contents similar to that of members of the Kengamine group (Takahashi *et al.,* 2008a). The Sen-nin group ranges from 62 to 66 wt% in SiO_2 content (silicic andesite to dacite) and has a higher MgO content than the Sekisonzan lava dome (Takahashi *et al*., 2008a). Based on whole-rock chemistry, especially the MgO content, the eruptive products of Kurofu volcano consist of three groups. These are, in order of increasing MgO content and ascending order of stratigraphy: (1) Gippa, (2) Kengamine-Sekisonzan, and (3) Mitsuone-Sen-nin. The volcanic rocks of Kurofu volcano are calc-alkaline and belong to the low-alkali tholeiite series and the low-to-medium-K series, except for some in the Gippa group, which are tholeiitic in composition (Fig. 27).

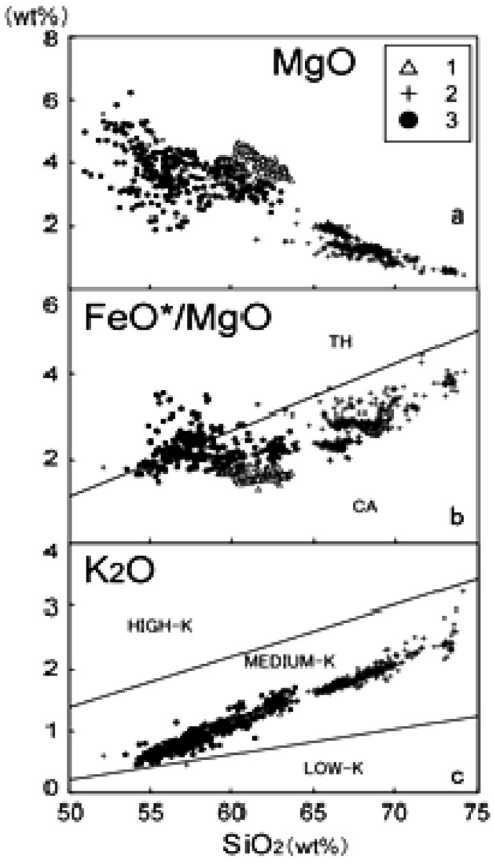

Fig. 27 SiO_2 variation diagram for eruptive products of Asama volcano. 1: Maekake volcano, 2: Hotokeiwa volcano, 3: Kurofu volcano, TH: tholeiitic rock series, CA: calc-alkalic rock series.

Hotokeiwa volcano

The rocks of the Hanareyama lava dome and the Kumoba pumice flow contain 65 to 75wt% SiO_2 and are characterized by low TiO_2 and MnO and high K_2O contents (Takahashi *et al.,* 2008b). The SiO_2 content of the Koasama lava dome and the Shiraito pumice fall varies from 65 to 73wt%, but that of

Koasama is restricted to 71 to 73wt% (Takahashi *et al.*, 2008b). The rocks of the lower member of the Hotokeiwa lava flows contain 69 to 74wt% SiO_2, and those of the first and second Okubozawa pumice falls and flows have 66 to 71wt% SiO_2 (Takahashi *et al.*, 2008b). The lower member of the Hotokeiwa lava flows and the first and second Okubozawa pyroclastic falls and flows show similar trends in silica variation diagrams; they are lower in MgO, FeO*, and CaO but higher in Al_2O_3 and Na_2O at the same SiO_2 content (Takahashi et al., 2008b). The Itahana yellow pumice and Tsumagoi pumice falls contain 62 to 70wt% SiO_2. The rocks of the first and second Komoro pumice flows consist of two clusters on the silica variation diagram; one corresponds to scoria and the mafic part of banded pumice and has 55 to 62wt% SiO_2, while the other is represented by pumice and has 65 to 70wt% SiO_2 (Takahashi *et al.*, 2008b). The middle member of the Hotokeiwa lava flows contains 69 to 72wt% SiO_2, and the upper member has about 59wt% (Takahashi *et al.*, 2008b). A middle member of the Hotokeiwa lava flows, the first and second Komoro pumice flows, shows a similar trend on the variation diagrams, but the Itahana yellow pumice and Tsumagoi pumice falls differ in composition; they are slightly lower in MgO, FeO*, and CaO but higher in Al_2O_3 and Na_2O contents at the same SiO_2 content.

The eruptive products of Hotokeiwa volcano and related monogenetic vents are divided into four groups on the basis of whole-rock chemistry, especially the MgO content. These are, in order of increasing MgO content: (1) the Kumoba pumice flow-Hanareyama lava dome-Koasama lava dome-Shiraito pumice fall-first and second Okubozawa pumice falls and flows-lower member of the Hotokeiwa lava, (2) the Itahana yellow pumice-Tsumagoi pumice falls, (3) the upper member of the Hotokeiwa lava, and (4) the first and second Komoro pumice flows-middle member of the Hotokeiwa lavas (Fig. 27). Most volcanic rocks of Hotokeiwa volcano and related pumice falls and flows belong to the low-alkali tholeiite, medium-K, and calc-alkaline rock series (Fig. 27).

Maekake volcano

The fallout products of Maekake volcano consist of at least ten large plinian ejecta. The SiO_2 contents of the eruptive products are as follows: As-A, Agatsuma pyroclastic flow and Onioshidashi lava flow (1783 A.D.), 60 to 64 wt%; As-B', 58 to 63 wt%; As-B, Oiwake pyroclastic flow and Kaminobutai lava flow (1108 A.D.), 59 to 61wt%; As-C, Shimonobutai lava flow (4C), 61 to 64wt%; As-D, 58 to 64wt%; As-E, 58 to 6 0wt%; and As-F, 58 to 63wt% (Takahashi et al., 2007). As-A is the highest in MgO and MnO and the lowest in Al_2O_3 and Na_2O, while As-B' and As-F are the lowest in MgO and MnO and the highest in Al_2O_3 and Na_2O. The compositions of several elements are clearly different between 1783 A.D. and 1108 A.D. eruptive products. The ejecta of the 1783 A.D. eruption are higher in MgO, FeO*, MnO, and CaO and lower in Al_2O_3 and Na_2O than those of the 1108 A.D. eruption (Fig. 28). All volcanic rocks of Maekake volcano belong to the medium-K and calc-alkaline rock series (Fig. 27).

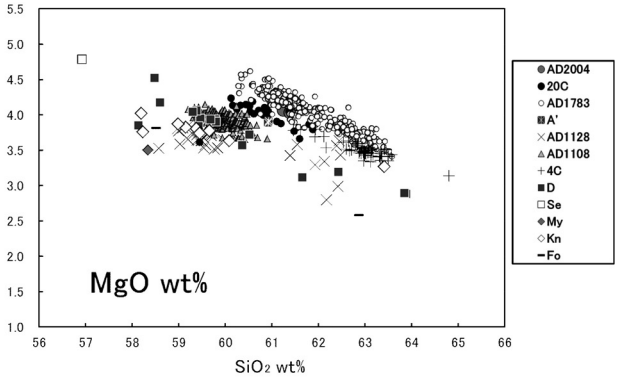

Fig. 28 Diagram of SiO_2 vs. MgO for volcanic rocks of Maekake volcano (Takahashi *et al.*, 2007). For details, see section 3-4.

5-3. Incompatible trace elements

In Asama volcano, the ratios of incompatible trace elements vary as the whole-rock SiO2 content increases. The Rb/Zr, Rb/Y, Rb/Ba, Ba/Y, and Zr/Y ratios increase from the basaltic andesite of the Gippa group to the dacite and rhyolite of Hotokeiwa volcano (Fig. 29); the ratios for the andesite of Kurofu, Hotokeiwa, and Maekake volcanoes lie between them, implying that it is difficult to derive andesite from basaltic andesite, as well as dacite-rhyolite from andesite, through simple crystallization differentiation. The ratio variation for the andesite of Asama volcano can be explained by the mixing of basaltic andesitic magma of the Gippa group with dacitic to rhyolitic magma of the Hotokeiwa volcano.

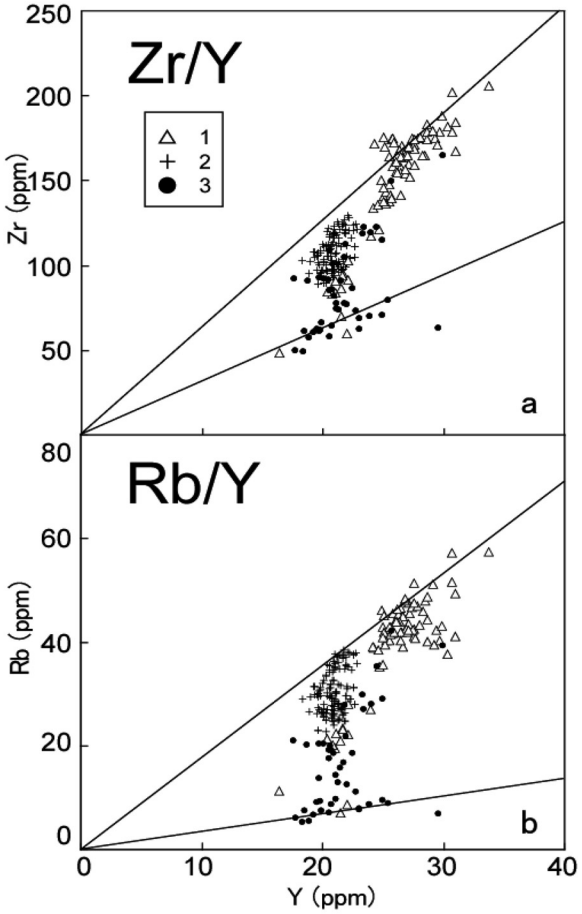

Fig. 29 Zr/Y and Rb/Y ratios for eruptive products of Asama volcano. 1: Maekake volcano, 2: Hotokeiwa volcano, 3: Kurofu volcano.

5-4. Magma mixing

Andesites of Asama volcano commonly show evidence of magma mixing (e.g., Miura, *et al*., 2004), including: (1) sieved texture of plagioclase, (2) bimodal distribution of core compositions of plagioclase, (3) reverse zoning of plagioclase and pyroxenes, (4) disequilibrium relations between olivine and pyroxenes, (5) linear distribution of whole-rock chemical compositions on SiO_2 variation diagrams, (6) several types of glass with different SiO_2 contents in the groundmass, (7) whole-rock incompatible trace element ratios, and (8) occurrence of banded pumice. Most andesites of Asama volcano are products of magma mixing.

(written by M. Takahashi)

6. Monitoring of Asama Volcano and its magma pathway

6-1. Overview of observation network at Asama volcano

Seismic observation at Asama volcano started in 1910, motivated by eruptions and seismic swarms in 1909 (Omori, 1912). This was one of the earliest seismic observations of an active volcano. The Imperial University of Tokyo and the Central Meteorological Observatory had conducted continuous seismic observations from 1911 to 1945. The Asama Volcano Observatory (AVO) was established in 1933 by Karuizawa town and donated to The Imperial University of Tokyo in 1934. After World War II, the seismic observations were resumed by the Earthquake Research Institute, University of Tokyo, and the Japan Meteorological Agency, which continue to conduct observations until now. A major achievement during the early days of seismic observation was the classification of volcanic earthquakes based on the observed waveforms by Minakami (1960). Although seismic observations in Asama volcano have been continuing for more than 100 years, there were only six seismometers in 1998. After 2003, a modern monitoring network was built to gain more insights into the internal structure of the volcano and the mechanics of magma transport beneath the volcano. The seismic network has grown rapidly since then, with 30 seismometers as of March 2012, 19 of which are equipped with broadband sensors (Fig. 30). Continuous GPS observations have been conducted in the Asama volcano region since 1996. As of 2012, there were 15 continuous GPS sites within 20 km of the summit, five within 4 km, and two on the rim of the summit crater (Fig. 31). There were also 10 tiltmeters, 13 microphones, and two cosmic ray muon detectors as of March 2012. On the west and east rims of the summit crater, small caves were located in which not only seismic and geodetic sensors but also other kinds of sensors, such as microphones, video and thermal cameras, and a detector of chemical components in volcanic gas, have been installed.

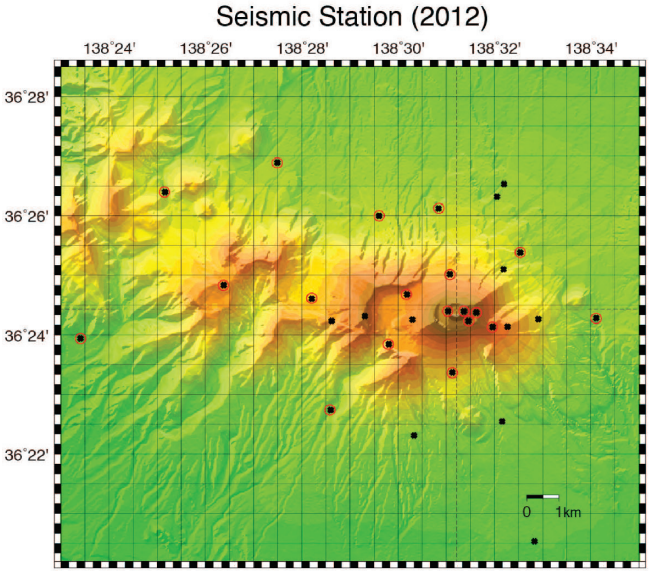

Fig. 30 Spatial distribution of seismometers as of March 2012. Red circles indicate broadband seismometers.

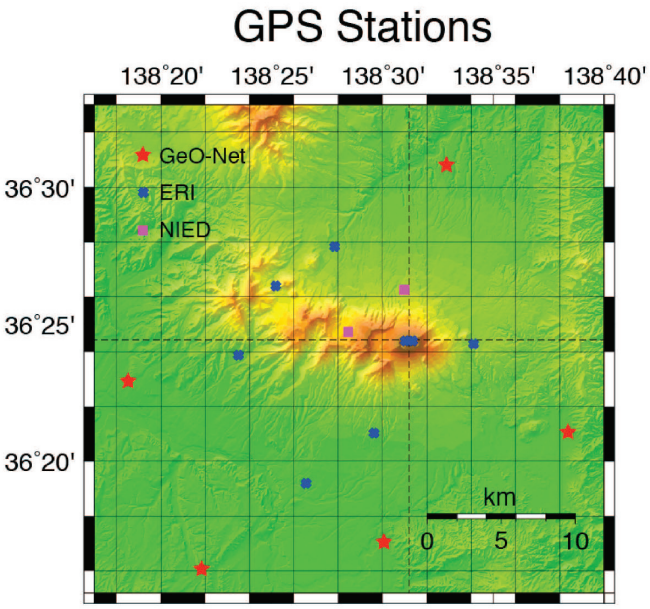

Fig. 31 Spatial distribution of GPS sites as of March 2012. Red stars, blue crosses, and pink rectangles denote those installed by the Geographical Survey Institute, Earthquake Research Institute, University of Tokyo, and the National Research Institute for Earth Science and Disaster Prevention, respectively.

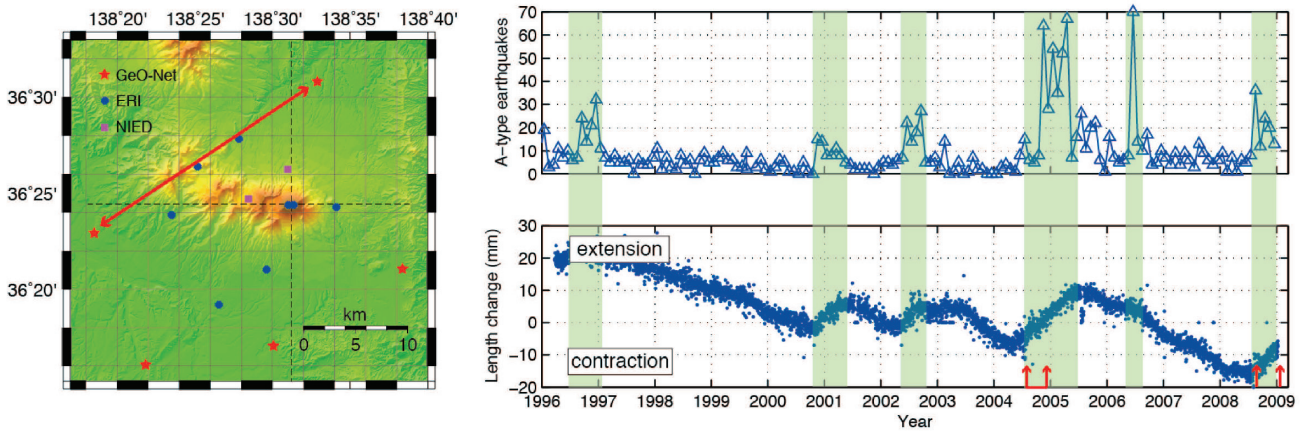

Fig. 32 Temporal evolution in monthly number of A-type (volcano-tectonic) earthquakes and ground deformation between 1996 and 2008. The GPS baseline length between 950221 and 950268 is obtained; both were installed by the Geographical Survey Institute, as shown in the map on the left. Red arrows indicate eruptions.

.

6-2. Overview of recent eruptions

6-2-1. Volcanic activities before 2004

Here, we provide an overview of the seismic and geodetic observations associated with unrest during the era of modern instrumentation since 1998, as well as the eruptions during that period. Figure 32

compares temporal variations in the monthly number of A-type (volcano-tectonic) earthquakes with the changes in the GPS baseline length between 950221 and 950268 from 1996 to 2009. The baseline extensions between these two GPS sites clearly indicate magma intrusions beneath the western flank of Asama volcano because the baseline crosses the inferred diking area, which is deduced from geodetic data during 2004 and 2008-2009 eruptions (Aoki *et al*., 2005; Takeo *et al*., 2006; Aoki *et al*., 2013). The hypocenter distribution before 2004 determined in the routine data processing by AVO indicates that the A-type earthquakes occurred under the western side of Asama volcano and that the other volcanic earthquakes occurred beneath the summit of Asama volcano; however, the processing precision was not as good as that after 2004 due to the lack of a dense seismic network. Because the inferred dike locations are associated with the extensions of the GPS baseline before 2004, and the subsequent eruptions in 2004, 2008, and 2009 are also to the west of the summit (Aoki *et al*., 2005; Murakami, 2005; Takeo *et al*., 2006), it seems reasonable to assume that the overall trend of hypocentral distribution and the dike location had not changed during the last decade. After 1998, the number of A-type earthquakes increased twice before the 2004 eruption, from October 2000 to April 2001 and from May 2002 to August 2002. Both seismic activations coincided with the extensions of the GPS baseline, suggesting that the A-type earthquakes were associated with the intrusion of magma beneath the western flank of Asama volcano.

On the other hand, contractions of the GPS baseline were also observed three times: prior to March 2000, from July 2001 to February 2002, and from March 2003 to April 2004. Because the observed contractions are too large to be explained by tectonic motion of nonvolcanic origin, we speculate that it might indicate migrations of intrusive magma from under the western flank of Asama volcano. Although the exact direction of the magma migration is unknown because the change in the GPS baseline length between 950221 and 950264 is sensitive only to the inflation and deflation under the western flank of Asama volcano, the magma may have migrated either vertically down to depth or eastward toward the vent at the time of the baseline contraction. The seismicity was relatively low during the first contraction period except for the last several months, while it remained at a high level during the latter two contraction periods. The maximum temperature of the crater had exceeded 200°C since autumn 2002 (Japan Meteorological Agency, 2005), suggesting that the shallow part of the vent had been at an elevated temperature from the middle of 2002. These observations suggest that there were certain essential differences between the first and later contractions. Continuous GPS data show that a sudden north-south extension of the volcano started in 21-22 July 2004, about 5 weeks before the first eruption of 2004. Volcanic glows had begun to be observed since the last ten days of July 2004, and the maximum temperature at the bottom of the crater exceeded 500°C after the sudden extension of the baseline length (Japan Meteorological Agency, 2005). These surface phenomena indicated that the temperature rise in the shallow part of the vent succeeded the magma intrusion.

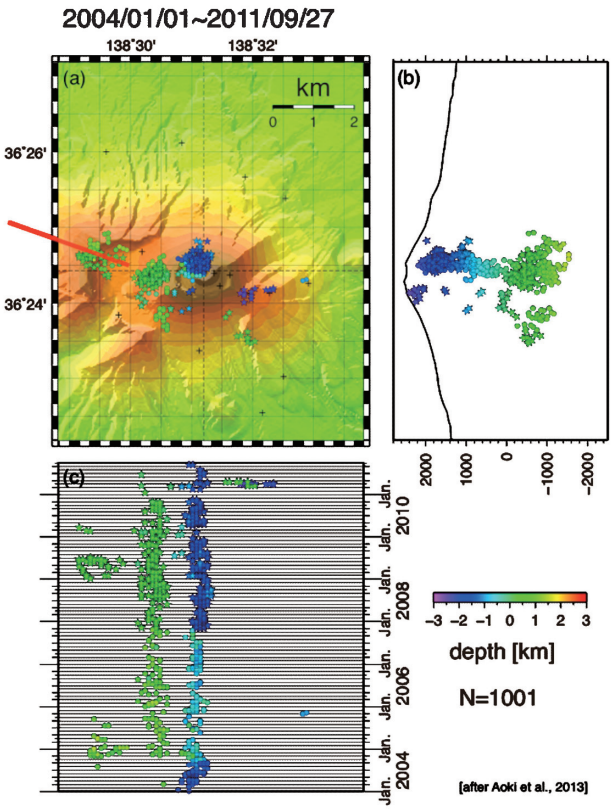

Fig. 33 Distribution of relocated hypocenters around Asama volcano between January 2004 and September 2011. Each hypocenter is colored according to its depth. (a) Distribution of epicenters with the approximate location of dike intrusions during crises (red line). (b) North-south cross section of hypocenters. (c) Temporal evolution of hypocenters. The horizontal axis represents the longitude of the hypocenters.

6-2-2. 2004 eruption

At 11:02 (GMT) on 1 September 2004, a moderate-sized vulcanian eruption (VEI 2) occurred for the first time in the last 21 years. The ash plume reached 3.5-5.5 km above the summit or 6-8 km above sea level. After a short period of quiescence, continuous strombolian eruptions started on 14 and 16-18 September before vulcanian eruptions occurred on 23 and 29 September, 10 October, 14 November, and 9 December. The total amount of ejected tephra is estimated to have been about 1.6 x 108 kg (Nakada *et al.,* 2005). The magma involved in the 2004 eruption was andesite, with a composition similar to magmas erupted over the past 10000 years.

Takeo *et al.* (2006) precisely relocated the hypocenters of more than 500 volcanic earthquakes between 1 January 2004 and 19 October 2005, spanning the period of the 2004 eruptions, using a double-difference algorithm (Waldhauser and Ellsworth, 2000). The relocated distribution reveals a sharp image of seismicity composed of two groups. One forms a WNW-ESE-directed zone at a depth range between 1 km and 1.5 km below sea level. The eastern end of this seismic zone lies beneath the summit crater and extends westward horizontally over 2 km in length. The other group forms a narrow vertical seismic zone extending from the eastern edge of the other group to just under the summit crater.

We also modeled the ground deformation field between June 2004 to March 2005 by inverting for length, width, depth, dip angle, strike direction, location, and amount of opening of an intruded rectangular dike in an elastic, homogeneous, and isotropic medium (Okada, 1985). Neither a spherical source nor a fault dislocation model explains the ground deformation pattern. The results show that the observations are well explained by a dike intrusion to the western flank of Asama volcano. The intruded volume was estimated to be 6.8 x 10^6 m^3 (Aoki *et al*., 2005; Takeo *et al*., 2006), which is about three times larger than the volume of emitted magma during the eruption (2 x 10^6 m^3; Nakada *et al.,* 2005). The eastern part of the dike overlaps with the western end of the relocated hypocenter distribution (Fig. 33). The depth at the top of the dike, with an estimated standard deviation of ±1.3 km, coincides with the depth range of the A-type earthquakes. The distribution of dike-induced seismicity reflects the distribution of ambient stresses that are near to failure; thus, the seismicity might be much more concentrated near the dike tip (Rubin *et al.*, 1998a; Rubin and Gillard, 1998b). The eastern end of the horizontally elongated seismicity is connected with the narrow vertical seismic zone, extending from 1 km below sea level to just under the eruptive summit crater (Fig. 33). We interpret this distribution of hypocenters as representative of the magma pathway beneath Asama volcano.

6-2-3. 2008-2009 eruption

After 4 years of repose, the seismic activity started to intensify in July 2008, one month before the first eruption in 2008. The earthquakes mainly occurred approximately 1 km to the west of the summit at about 1 km below sea level (Fig. 33). The seismicity increased on 8 August, leading to eruptions on 10, 11, and 14 August. Since September 2008, the enhanced seismicity has been observed 2 km to the west of the summit at 1 km below sea level (Fig. 33). On 1 February 2009, the seismicity just beneath the summit crater increased (a tiltmeter located about 3 km from the summit tilted away from the volcano), leading to a summit eruption the next day. Minor eruptions from the summit occurred intermittently on 9-16 February, 15 March, 14 and 30 April, and 3 and 27 May, with a plume height of less than 500 m. The ejected mass due to the eruption on 2 February was 2.0-2.4 x 10^7 kg, approximately 20% of that associated with the 1 September 2004 eruption (Maeno *et al*., 2010).

The western side of the volcano started to exhibit a north-south extension from July 2008, a month before the first eruption in 2008 (Fig. 32). The volcano then expanded quasi-linearly until June 2009. This extension was due to dike intrusion to the west of the summit, as in the 2004 case. The displacement field between June and December 2008 is fitted well by an east-west-directed dike with its top at 0.7 km below sea level and a shallow source responsible for the summit inflation. The east-west-directed dike lies near the one involved in the 2004 activity, indicating that the dike intrusion to the west of the summit is ubiquitous during the unrest of Asama volcano. This also implies the presence of an established magma pathway to the west of the summit. The volume of intrusion is estimated to be 1.64 x 10^6 m^3, approximately 25% of that during the 2004 activity.

6-3. Location of magma chamber in the upper crust

A regional seismic tomography study images broader-scale structures from the lower crust to the upper mantle but is not capable of imaging the upper

crust in detail. Nagaoka *et al*. (2012) used seismic ambient noise to image the seismic structure of the upper crust beneath Asama volcano. First, they divided the whole region into three subregions according to a priori knowledge. Using 89 vertical seismograms around Asama volcano, they took the cross-correlations of all possible pairs within each subregion. The obtained cross-correlations show the propagation of the Rayleigh wave trains in all subregions but with different speeds. In each subregion, the reference dispersion curves were measured with the assumption that the seismic structure varies only with depth within each subregion. Once the reference phase velocity had been obtained, the travel time anomaly was measured as a perturbation from the reference phase velocity for all available station pairs. An iterative nonlinear inversion (Rawlinson and Sambridge, 2003) was applied to estimate the phase velocities of a given frequency range at grid points with a spacing of 0.03 degree. The spatial variations of the Rayleigh wave phase velocity at a frequency of 0.1-0.2 Hz showed a negative velocity anomaly of up to ~ 20% to ~ 10 km west of the summit (Fig. 34a).

The regionalized dispersion curves were inverted for local 1-D velocity models at each point (Montagner, 1986). Figure 5.5.b shows the 3-D S-wave tomographic model from a collection of the local 1-D S-wave velocity structures. This figure indicates a low S-wave velocity at depths of 5-10 km (enclosed by a red circle in Fig. 34b) and high S-wave velocity anomalies at shallower depths (< 3 km) around the repeated diking region inferred from an active source seismic exploration (enclosed by a blue ellipse in Fig. 34b) (Aoki *et al.*, 2009). The S-wave velocity structure is consistent with the P-wave velocity derived from the seismic exploration.

What causes the low S-wave velocity to change from 5 to 10 km? We observed tilt motions during the February 2009 eruption, many of which were obtained from the horizontal record of broadband seismometers. Excluding the tilt records from sites near the summit, the other sites generally tilt toward the west of the summit by up to 1.1 μrad, which imply a source offset to the west. The observed deformation field is well explained by a deflating embedded dike at its top at about 1 km below sea level with a NW-SE strike, the location of which is right above the low S-wave velocity anomaly. The existence of a dike participating in an eruption suggests that the low S-wave velocity anomaly represents the magma chamber beneath the dike deflating during the 2009 eruption. Because of technical difficulties, the crustal magma chamber has not been imaged at all (Aoki *et al.,* 2009), except as a broad low-velocity zone (Lees, 2007) in conventional seismic imaging studies. Therefore, this study is the first to delineate the size of the crustal magma chamber.

6-4. Synthesis

Together with the discussions above, in Figure 34c we represent a synthesis of the magma pathway in the upper crust beneath Asama volcano based on our observations. When magma rises to the upper crust, it is stored in the magma chamber at a depth of 5-10 km. The magma chamber is offset by approximately 8 km to the west from the summit and is represented by a low-velocity region. Then the magma further moves up to a depth of about 1 km below sea level as a dike. The shallow seismic and resistivity structures (Aizawa *et al*., 2008; Aoki *et al*., 2009) suggest that the magma pathway is subject to structural controls to form a winding path to reach the surface. Combining these multiple constraints enables us to gain a unified understanding of the magma plumbing system of Asama volcano from the crustal magma chamber to the surface.

(written by M. Takeo and Y. Aoki)

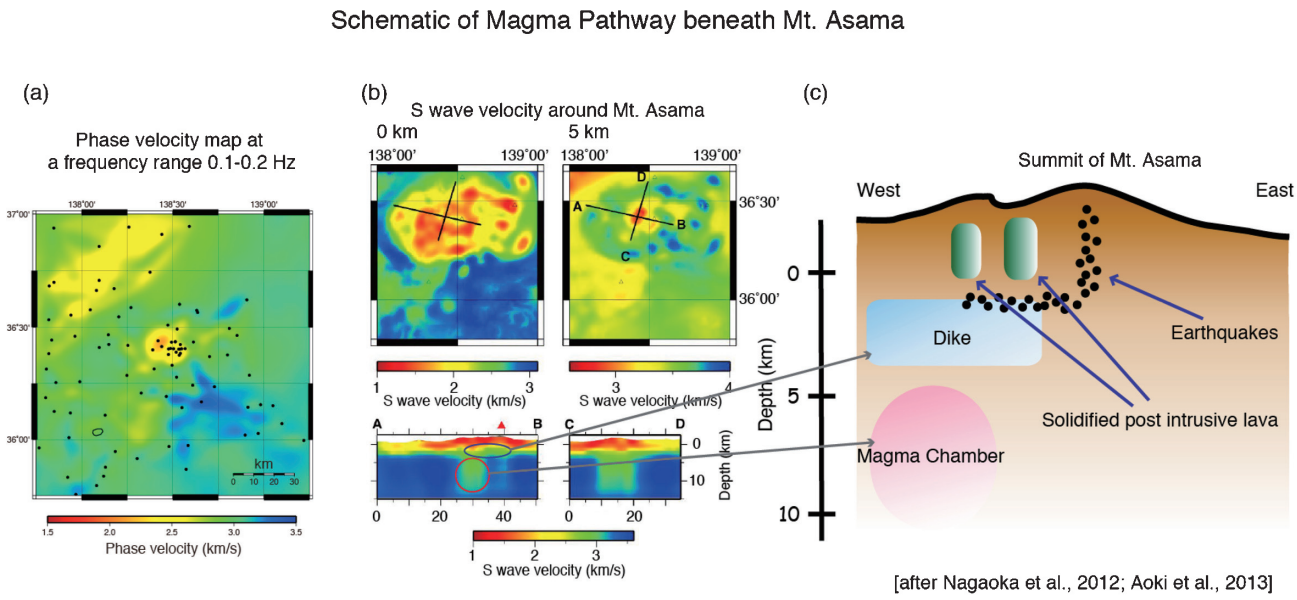

Fig. 34 Schematic of the magma pathway beneath Asama volcano. (a) The obtained Rayleigh wave phase velocity map at a frequency range of 0.1-0.2 Hz. (b) The shear wave velocity around Asama volcano. The upper panels represent the plan view of the S-wave velocity at depths of 0 and 5 km, respectively. The lower panels represent the vertical view of the S-wave velocity along the A-B and C-D baselines, respectively, shown in the upper panels. (c) Schematic of the magma pathway integrating seismic and geodetic observations.

7. Volcanic hazards and mitigation of volcanic disasters

7-1. Small-scale eruptions

The characteristic features of the explosive eruptions of Asama volcano have been closely monitored since 1911, when a small observatory (the first volcano observatory in Japan) was founded on the western slope of the volcano. Since then the volcano has been closely monitored and scientifically investigated. The period 1911-1973 was characterized by frequent, violent vulcanian activities, but since then up to the present, the volcano has stayed very calm with very few minor explosions. The activity reached its peak during 1930-1983; in particular, 398 explosions occurred within a one-year period in 1941. The largest explosions scattered large bread-crust bombs within a radius of 4 km, but no single eruption exceeded 500,000 tons of ejecta by weight, corresponding to VEI 2. The shock waves associated with the explosions could break the window glass of buidings as far as 15km from the summit. The ash plumes could rise as high as several thousand meters and could deposit a thin ash layer as far as more than 100 km downwind. Not infrequently, minor pyroclastic flows occurred from the partial collapse of the column, reaching a few kilometers from the crater.

To cope with this magnitude of hazards, a circular off-limits zone with a 4km radius has been established around the summit crater; except for mountain trails, no roads are constructed in this zone. If the magnitude of precursors, such as volcanic earthquakes and edifice inflation, is minor, the Japan Meteorology Agency (JMA) sets the alert level to 1 and declares a 500m-radius off-limits zone. If the alert level is raised to 2, the off-limits radius is increased to 2km from the crater. At the highest alert level of 3, the off-limits zone is 4km from the crater, which is the highest expected hazards magnitude applicable considering the past 120 years of vulcanian activity of the volcano. The alert level 4 indicates immediate danger of devastation in the inhabited area so the inhabitants are advised to prepare for immediate evacuation. Level 5 means the eruption has actually started or the devastation is foreseen; thus, it calls for immediate evacuation. So far, levels 4 and 5 have never been declared since the alert system was established in 2010. Before the end of World War II, at least 45 casualties of eruption had been recorded; these people died within a radius of 4km from the summit crater. In the last 50 years that the volcanic alert system has been enforced, there has been no casualty.

7-2. Lahar hazards produced by melting of snow by pyroclastic flows

Lahar hazards are expected when the higher slopes of the volcano are covered by snow and ice.

Pyroclastic flows and surges, despite being small in scale and not reaching the inhabited area, may cause melting of ice and snow, thus generating lahars. Local authorities and the JMA have agreed to issue an alert in case pyroclastic flows are observed during winter time, when substantial snow and ice are present in the summit area. Based on numerical simulations of possible lahar generation, hazard maps of lahars following several important ravines running through inhabited areas have been prepared and evacuation programs established.

7-3. Large-scale eruptions

The youngest member of the volcanic edifices that make up Asama volcano is Maekake-yama. This volcano is estimated to be around 10,000 years old, but it has been monitored by modern technology only in the last 120 years. The written documents before this period are sporadic and unreliable; thus, the exact profile of the past activity of Maekake-yama remains very vague. From the tephrochronology, it is known that 8 to 10 major plinian eruptions have taken place from the summit crater of Maekake-yama. The latest two of these, the eruptions of 1783 and 1108, both with a magnitude of VEI 4, are the most closely studied. As described in the foregoing, these two eruptions ejected ca.8 – 20 x 10E8 tons of magma by weight. This means that the magnitude gap between these two large-scale eruptions and the vulcanian eruptions in the last 120 years amounts to 10E3 (1000 times), which leaves us without any knowledge of the past intermediate-size eruptions of Maekake-yama.

In any case, the 11 March 2011 earthquake-tsunami disasters in Tohoku, Japan, spurred a general effort toward disaster management planning for unexpected large-scale events. The local communities surrounding Asama formed a joint consortium to prepare an overall disaster mitigation management program to deal with large-scale eruptions in the future. The effort included national government offices, such as the JMA; the Cabinet office; the Ministry of Land, Infrastructure, Transport and Tourism; and the prefectural governments of Nagano and Gunma. After completing a mitigation program regarding lahars, the task group has started to deal with large-scale eruptions, such as those that occurred in 1783 and 1108.

It is very difficult to tackle such an emergency management program because most people have never encountered a large-scale volcanic eruption, which happens once every hundred or thousand years.

Plinian fallout: Following the 1783 and 1108 eruptions, in both of which plinian pyroclastic falls played an important role in devastating wide areas at the eastern foot of the volcano, an evacuation plan covering the eastern foot should be planned. The threshold thickness of fall deposit that would trigger a mass evacuation is unknown to any specialist, as is the physical damage of the ash fallout, especially on highly developed urban areas. In addition, preparing a community security strategy is a challenge.

Pyroclastic flows: In both the 1783 and 1108 eruptions, pyroclastic flows also presented a serious threat. The flows in both cases covered wide areas of the southern and northern slopes to depths of a few to more than 30 meters. Pyroclastic flows will be the largest menace to residents who live closer to the volcano (say, within 20 km from the summit), and the overall strategy of disaster management, including the setting up of operation centers, will be very difficult.

Lava flows: Andesitic lava flows will be rather slow to advance over the lower slopes of the volcano and thus will present no immediate threat to human lives. In the past eruptions, the lava flows did not extend longer than 6 km from the vent.

Lahars and debris flows: Various kinds of debris flows may be expected to occur during and after a major eruption. In the 1783 eruption, a special type of debris flow/avalanche devastated the northern slopes and the river downslope, killing about 1500 people and damaging more than 1000 houses. A distinct alert for this kind of debris flow should be considered. Ordinary lahars and debris flows combined with ash fallout and torrential rainfall may be the most frequent hazards during and after a major eruption.

In the next few years, the general disaster mitigation plan for large-scale eruptions of Asama volcano is expected to be implemented.

(written by S. Aramaki)

Description of field trip stops

Day 1
Komoro
The pumice flow deposits of Hotokeiwa volcano are widely distributed on the southern and the northern foot of the volcano. In particular, the district of Komoro has a well-preserved plateau of the pumice flow deposits. During the field trip, we will observe the occurrence of the massive pumice flow deposits.

Stop 1-1: A cliff in front of Gymnasium Komoro
A well-preserved sequence of the pumice flow deposits is exposed on the cliff at Stop 1-1. It includes several flow units and ashfall layers.

Stop 1-2:Minamijo park
The boundary between the first and second Komoro pumice flow deposits can be observed in Minamijo park. Black soil of about 20cm thickness is visible between the two deposits. Gas segregation pipes are distinct in the pinkish, non-welded first Komoro pumice flow deposit. Nearby *Kaikoen*, a memorial park of the 16th century Komoro castle, stands on the plateau and alongside Chikuma River.

Stop 1-3: Hoshou
The topography of the box canyon called *Tagiri*, which is a typical erosional topography of the non-welded pumice flow deposit, can be observed around Stop 1-3.

Day 2
Mt. Kurofu
Stop 2-1: Kurumazaka pass
Kurumazaka pass, located at the altitude of 2000 m, is a horseback riding trail between the volcanoes Kurofu and Takamine. A fault that cuts through Kurofu volcano can be seen on the east (Fig. 4).

Stop 2-2: Tomi-no-kashira – viewing stop just below the summit of Mt. Kurofu
The excursion will reach the edge of a gigantic horseshoe-shaped crater formed by a sector collapse in ca. 23ka. The internal structure of Kurofu volcano and the pyroclastic cones of Maekake and Kamayama can be seen from Stop 2-2 (Fig. 35).

Stop 2-3: Ikenotaira marsh (optional)
Stop 2-3 is a volcanic crater of Sanpogamine volcano (Fig. 2a). A marsh called *Ikenotaira* has developed in the crater and is famous for hiking.. Although the correlative tephra fall deposits are unknown, the 1km-diameter crater is believed to be the site of explosive eruptions in the past.

Fig. 35 Pyroclastic cones of Maekake and Kamayama seen from the west (Stop 2-2). A collapsed cliff of Mt. Kurofu is shown in the lower left-hand portion.

Day 3
Eastern flank of Asama-Maekake volcano
Stop 3-1: Parking area (Kuromame-gawara) – overview of Asama and nearby volcanoes and the pyroclastic flow deposit of the 1783 eruption
The parking area is located on the northeastern flank of Asama and offers an excellent view of Maekakeyama and its lower slopes. To the left, the Koasama lava dome and thick lava flows of the Hotokeiwa stage can be seen. Note the relatively gentle slope defined by the Hotokeiwa lava. Tracing the skyline to the summit, one will find that the gradient of the slope steepens at the meeting point between two volcanic edifices, Hotokeiwa and Maekake. Kamayama cannot be seen from here, but the highest point, where smoke may be rising, is the location of its summit crater. To the right, the jagged skyline is remarkable, formed by the 1783 lava flow that flowed down the northern slope of Maekake and then branched to the northeastern slope. Two step-like surfaces of lava flows can be recognized below the NE branch of the 1783 lava: the upper one (Kaminobutai lava) formed in the 1108 A.D. eruption and the lower one (Shimonobutai lava) formed in the 4th century. The field of the 1783 pyroclastic flows has little vegetation and spreads out in front toward the upper slope of the volcano. This parking area is also built on the pyroclastic flow deposit. Because the original depositional surface of the flow units (e.g., lobes bounded by levees) is well preserved, the

boundaries of these units can be identified from aerial photographs. Also, to the east, north, and west, the volcanic morphology of the surrounding terrain can be observed.

Near the parking area is a dry ravine, along which a section of the pyroclastic flow deposit of the 1783 eruption is well exposed. The thickness of the deposit is about 1.5m. The deposit is strongly welded, and rough joints have developed. A reddish-brown, oxidized zone is distinguishable in the uppermost part of the deposit. Scoriaceous blocks with a characteristic cabbage-like shape are contained in the matrix. Below the pyroclastic flow deposit, the pumice fall deposit of the 1783 eruption can be recognized.

Stop 3-2: Asama-en, the museum – the 1783 lava flow

Pause to view the lava from the entrance of the trail in Asamae. Just in front, a large depression on the lava can also be seen. The lava flow cascaded down to the depression and continued to flow to the north. The complicated distribution of the flow units of lava around here has been described by Inoue (1998). The field trip includes a hike along the trail to see the surface features of the lava. In particular, welded features, such as flattened oxidized spatters, are characteristic; non-welded parts composed of reddish scoria and ash can sometimes be seen, indicating that the lava is clastogenic.

A borehole core, which penetrated through the lava from the bottom of the depression, provides a detailed view of the internal structure of the lava. The thickness of the flow is 64 m, and extensive welded features, such as eutaxitic texture and abundant broken crystals, can be recognized throughout the core.

The origin of the depression is also a point of discussion because the Kambara pyroclastic flow/debris avalanche deposit seems to have converged at this depression and not at the summit crater.

Stop 3-3: "Prince Land," subdivisions for holiday homes – gigantic blocks of the 1783 Kambara pyroclastic flow deposit

The field trip includes a visit to "Prince Land," where gigantic blocks up to tens of meters long are scattered. Most blocks have a rather flattened outline, and chilled margins are often observed. Open cracks on the surface, which are similar to those on bread-crust bombs, are sometimes found, suggesting in-situ plastic deformation. On the basis of these observations, Aramaki (1956) concluded that these blocks were emplaced at high temperatures. The blocks quite mimic the 1783 lava in terms of the occurrence of welded features. Sometimes, a change in the degree of welding within a single block can be seen.

Stop 3-4: Kambara village – the observational points around the Kannondo Temple

The excavated 35 stone steps, which were under the bridge that passed between the highest step and the 15th step, have been reburied for safety reasons. Some gravestones for those killed by the Kambara pyroclastic flow/debris avalanche stand to the right of the stone steps, with engravings indicating the year 1783.

A large stone tower with the names of the 466 victims stands to the left of the entrance to the Kannondo Temple (Fig. 36). The Buddhist names on the stone often include characters such as “water” and “mud,” indicating the devastating cause of these people’s deaths. A stone shrine to the right of the entrance to the Kannondo Temple is engraved with the words “The Enmeiji Temple in Mt. Asama,” indicating the name of the temple. This stone shrine was transported to the riverbed about 25 km downstream from Kambara village by the sand flow caused by the eruption. It was later relocated back to Kambara village. The Enmeiji Temple was previously located about 100 m north of the Kannondo Temple. The excavation of this site recovered facilities such as temples and storages. In addition, the details of the religious and daily lives of villagers are reflected by the excavated utensils, including Buddhist items, kettles, bowls, and plates. The temple is now located on a green tract of land.

Next to the Kannondo Temple is a village museum that exhibits the excavated artifacts from Kambara village. The museum also displays a topographic figure of the northern landscape of Mt. Asama showing the geographic location of the village, as well as the reconstructed faces of the two victims found at the stone steps of the Kannondo Temple (Fig. 37). Moreover, the Buddhist items and horse bones excavated from the Enmeiji Temple and the utensils recovered around the temple are displayed to provide insights into the lives of people in those days. This museum also exhibits replicated drawings of the mudflow disaster along the rivers.

Fig. 36 The large stone tower engraved with the names of the 677 victims of the 1783 eruption.

Fig. 37 The reconstructed faces of the victims excavated from the stone steps of the Kannondo Temple (Tsumagoi Village Museum).

Day 4

Stop 4-1: Ko-Asama lava dome

Koasama (Little Asama) is a lava dome that erupted on the eastern slope of Asama volcano. Its age is estimated to be 18ka. Because the lava dome is covered by thick tephra of a younger age, the exposure of the dome lava is restricted to the summit area. Ranging from grayish to pinkish, the massive lava shows a rhyolitic composition with 71-73% SiO2 and has a small amount of plagioclase and pyroxene phenocrysts. A small depression on the summit is considered to be a fault (Aramaki, 1963). The trip involves a moderate hike from the observatory to the dome. A climb to the summit of the dome presents a clear view of the surrounding area. Note, in particular, the devastated area to the north caused by the pyroclastic flows throughout the 1783 eruption.

Stop 4-2: Asama Volcano Observatory – the 1783 pyroclastic fall deposits

The observatory is located about 4 km due east of the active crater at 1,406 m above sea level. It was inaugurated in 1935 and is now a branch of the Earthquake Research Institute, University of Tokyo, with a new wing and a tower added in the 1980s. Although the volcano is in a quiet mood at the moment, the telemetered network constantly collects real-time data on earthquakes, ground tilt, temperature, and other parameters.

The field trip includes an observation of the pyroclastic fall deposits of the 1783 eruption through a pumice rock cut to more than 1.5 m thick at the observatory. The ESE pyroclastic fall deposits consist of twenty-two fall units of pumice and ash. The deposit is characterized by a lower, stratified half and an upper, massive half. The lower half consists of many thin (up to 10 cm), fine-grained pumice fall units: Layers, 2p-4p, 6p-9p, 11p, 13p, 15p-16p, and 17p. Layer 19p in the middle level is coarser than the underlying units (Fig. 38). The upper half (Layer 21p) is composed of a single massive layer, although it may show weak stratification at some localities. Layer 21p is the thickest and coarsest-grained, occupying more than half of the total volume. From the large volume and the column height estimates, Layer 21p is considered to be the product of the plinian eruption in the climactic phase (i.e., the final phase of Episode 5). It has also been suggested that most of the lower half of the ESE pyroclastic fall deposits corresponds to the intermittent plinian eruptions from 2 to 4 August (i.e., the earlier phases of Episode 5). For details, see section 3-2.

The ESE pyroclastic fall deposits contain several fine-ash layers: 1a, 5a, 10a, 12a, 14a, 18a, 20a, and 22a. We will also discuss the origin of these ashfall deposits.

Stop 4-3: Shiraito Falls

The field trip includes a visit to Shiraito Falls, one of the most popular sightseeing spots in Asama (Fig. 39). Here, the groundwater flows above and through the pumice fall deposit to form a unique waterfall. The age of this pumice fall (As-SP) has not been explicitly determined. The shape of the isopach map for this pumice fall deposit converges to an area that is now occupied by the Koasama lava dome. Therefore, it is believed that a plinian eruption might have occurred first, followed by the extrusion of a lava dome.

Fig. 38 Pumice cut at the Asama Volcano Observatory.

Fig. 39 Shiraito Falls.

References

Aizawa, K., Ogawa, Y., Hashimoto, T., Koyama, T., Kanda, W., Yamaya, Y., Mishina, M., and Kagiyama, T. (2008) Shallow resistivity structure of Asama volcano and its implications for magma ascent process in the 2004 eruption. *J. Volcanol. Geotherm. Res.*, **173**, 165-177, doi: 10.1016/j. jvolgeores. 2008.01.016.

Aoki, Y., Watanabe, H., Koyama, E., Oikawa, J., and Morita, Y., (2005) Ground deformation associated with the 2004-2005 unrest of Asama Volcano, Japan. *Bull. Volcanol. Soc. Japan,* **50**, 575-584. (in Japanese with English abstract).

Aoki, Y., Takeo, M., Aoyama, H., Fujimatsu, J., Matsumoto, S., Miyamachi, H., Nakamichi, H., Ohkura, T., Ohminato, T., Oikawa, J., Tanada, R., Tsutsui, T., Yamamoto, B.L.N., Yamamoto, M., Yamasato, H., and Yamawaki, T. (2009) P-wave velocity structure beneath Asama Volcano, Japan, inferred from active source seismic experiment. *J. Volcanol. Geotherm. Res.*, **187**, 272-277, doi: 10.1016/j.jvolgeores.2009.09.004.

Aoki, Y., Takeo, M., Ohminato, T., Nagaoka, Y., and Nishida, K., (2013) Magma pathway and its structural controls of Asama Volcano, Japan. *Geological Society, London, Special Publications*, **380**, doi 10.1144/SP380.6.

Aramaki, S. (1956) The 1783 activity of Asama volcano. Part I. *Jap. J. Geol. Geogr,.* **27**, 189-229.

Aramaki, S. (1957) The 1783 activity of Asama volcano. Part II. *Jap. J. Geol. Geogr.*, **28**, 11-33.

Aramaki, S. (1963) Geology of Asama volcano. *J. Fac. Sci. Univ. Tokyo*, sec.2, **14**, 229-443.

Aramaki, S. (1993) Geological map of Asama Volcano. Geolgical Map of Vocanoes, 6, Geological Survey of Japan.

Aramaki, S. and Hayakawa, Y. (1982) Ash-fall during the April 26, 1982 eruption of Asama volcano. *Bull. Volcanol. Soc. Japan.* **27**: 203-215. (in Japanese with English abstract).

Aramaki, S. and Takahashi, M. (1992) Geology and petrology In: Guide book for field workshop at Asama and Kusatsu-Shirane volcanoes, Japan. IAVCEI Commission on Explosive Volcanism, 40p.

Asama Jomon Museum (2004) Catalog of exhibition on the eruption of Mt. Asama in 1783. 95p. (in Japanese).

Gunma Archaeological Research Foundation (2011) Excavation report of the Higashimiya site, 1. 484p. (In Japanese).

Gunma Prefectural Museum of History (1995) Catalog of exhibition on the eruption of Mt. Asama in 1783. 91p. (in Japanese).

Inoue, M. (1998) Structure of the Onioshidashi lava flow of Asama volcano. Master's Thesis, Kanazawa Univ., 70p.

Inoue, K., Ishikawa, Y., Yamada, T., Yajima, S., and Yamakawa, K. (1994) Distribution and mode of the Kambara pyroclastic flow-cum-mudflow of the 1783 eruption in Asama volcano. *J. Jap. Soc. Engineering Geol.,* **35,** no.1, 12-30. (in Japanese with English abstract).

Japan Meteorological Agency (2005) Abstract of volcanic activities of Asamayama in 2004. *Report of Coordinating Committee for Prediction of Volcanic Eruption*, no. 89, 11-23.

Kaneko, T., Shimizu, S. and Itaya, T. (1989) K-Ar chronological study of the Quaternary volcanic activity in Shin-Highland. *Jour. Miner. Petrol. Econ. Geol*., **84**, 211-225.

Lees, J.M. (2007) Seismic tomography of magmatic systems. *J. Volcanol. Geotherm. Res.,* **167**, 35-56, doi: 10.1016/j.jvolgeores. 2007.06.008.

Maeno, F., Suzuki, Y., Nakada, S., Koyama, E., Kaneko, T., Fujii, T., Miyamura, J., Onizawa, S., and Nagai, M. (2010) Course and ejecta of the eruption of Asama Volcano on 2 February 2009. *Bull. Volcanol. Soc. Japan,* **55**, 147-154. (in Japanese with English abstract).

Minakami, T. (1942a) On the distribution of volcanic ejecta. (Part 1.) The distribution of volcanic bombs ejected by the recent explosions of Asama. *Bull. Earthq. Res. Inst.,* **20**, 65-92.

Minakami, T. (1942b) On the distribution of volcanic ejecta. (Part II) The distribution of Mt. Asama pumice in 1783. *Bull. Earthquake Res. Inst., Univ. Tokyo,* **20**, 93-106.

Minakami, T. (1960) Fundamental research for predicting volcanic eruptions (Part 1). *Bull. Earthq. Res. Inst., Univ. Tokyo,* **38**, 497-544.

Montagner, J.-P. (1986) Three-dimensional structure of the Indian Ocean inferred from long period surface waves. *Geophys. Res. Lett.,* **13**, 315-318, doi: 10.1029/GL013i004p00315.

Murakami, M. (2005) Magma plumbing system of the Asama volcano inferred from continuous measurements of GPS, migration preceding 2004 eruption of Asama Volcano detected by GPS. *Bull. Volcanol. Soc. Japan,* **50**, 347-361. (in Japanese with English abstract).

Nagaoka, Y., Nishida, K., Aoki, Y., Takeo, M., and Ohminato, T. (2012) Seismic imaging of magma chamber beneath an active volcano. *Earth Planet. Sci. Lett.,* 333-334, 1-8, doi: 10.1016/j.epsl. 2012.03.034.

Nakada, S., Yoshimoto, M., Koyama, E., Tsuji, T., and Urabe, T. (2005) Comparative study of the 2004 eruption with old eruptions at Asama Volcano and activity evaluation, *Bull. Volcanol. Soc. Japan,* **50**, 303-313. (in Japanese with English abstract).

Nakajima, J. and Hasegawa, A. (2007) Subduction of the Philippine Sea plate beneath southwestern Japan: Slab geometry and its relationship to arc magmatism. *J. Geophys. Res.,* **112**, B08306, doi: 10.1029/ 2006JB004770

Nakamura, T., Tsuji, S., Takemoto, H., and Ikeda, A. (1997) 14C age measurements with accelerator mass spectrometry of Asama Tephra stratigraphic samples around Minami-Karuizawa, the Latest Pleistocene, Nagano Prefecture, central Japan. *Jour. Geol. Soc. Japan.* **103**, 990-993. (in Japanese with English abstract).

Okada, Y. (1985) Surface deformation due to shear and tensile faults in a half-space, *Bull. Seism. Soc. Am.,* **75**, 1135-1154.

Omori, F. (1912) The eruptions and earthquakes of the Asama-yama, *Bull. Imperial Earthquake Investigation Committee,* **6**, 1-147.

Rawlinson, N., and Sambridge, M. (2003) Irregular interface parameterization in 3-D wide-angle seismic traveltime tomography, *Geophys. J. Int.,* **155**, 79-92, doi: 10.1146/J.1365-246X. 2003.01983.x.

Rubin, A. M., and Gillard, D. (1998) Dike-induced earthquakes: Theoretical considerations. *J. Geophys. Res.,* **103**, 10,017-10,030.

Rubin, A. M., Gillard, D., and Got, J-L. (1998) A reinterpretation of seismicity associated with the January 1983 dike intrusion at Kilauea Volcano, Hawaii, *J. Geophys. Res.,* **103**, 10,003-10,015.

Seki, T. (2010) The archaeological sites destroyed by the eruption, Shinsensha. 93p. (in Japanese).

Shimozuru, D. (1981) The structure of the ENE

flank of Asama volcano determined by geophysical methods. In Aramaki, S. (ed) Asama yama, Report of the special research on natural hazards assisted by the Ministry of Education, Japan, 82-87.

Takahashi, K. and Miyake, Y. (2004) K-Ar Ages of Lavas from the Mount Eboshidake, Johshin District, Central Japan. *Bull. Volcanol. Soc. Japan,* **49**, 207-212. (in Japanese with English abstract).

Takahashi, M., Yasui, M., Ichikawa, Y., Kamioka, Y., Asaka, N., Sakagami, M. and Tanaka, E. (2007) Whole-rock major element chemistry for eruptive products of Asama-Maekake Volcano, central Japan: Summary for data of 288 samples. *Proc., Inst. Nat. Sci. Nihon Univ.,* **42**, 55-70. (in Japanese with English abstract).

Takahashi, M., Nakajima, T., Mukai, Y., Yasui, M. and Kanamaru, T. (2008a) Major element chemistry for eruptive products of Asama-Kurofu Volcano, central Japan: Summary for data of 288 samples. *Proc., Inst. Nat. Sci. Nihon Univ.*, **43**, 195-216. (in Japanese with English abstract).

Takahashi, M., Mukai, Y., Nakajima, T., Yasui, M. and Kanamaru, T. (2008b) Major element chemistry for eruptive products of Asama-Hotokeiwa Volcano, central Japan: Summary for data of 307 samples. *Proc., Inst. Nat. Sci. Nihon Univ.,* **43**, 167-193. (in Japanese with English abstract).

Takahashi, M., Otsuka, T., Hirakawa, T., Nagai, M., Yasui, M. and Aramaki, S. (2013) Whole-rock major element chemistry for eruptive products of the Eboshi volcano group, central Japan: Summary 222 analytical data. *Proc., Inst. Nat. Sci. Nihon Univ.,* **48**, 111-140. (in Japanese with English abstract).

Takemoto, H. (1999) Paleoenvironmental change and volcanic activities in the north-western part of northern Kanto. Ph.D. Dissertation, Ibaraki Univ. 1-128p. (in Japanese).

Takeo, M., Aoki, Y., Ohminato, T., and Yamamoto, M. (2006), Magma supply path beneath Mt. Asama volcano, Japan. *Geophys. Res. Lett.,* **33**, L15310, doi: 10.1029/2006GL026247.

Tanaka, E., Yasui, M. and Aramaki, S. (2012) Nature of the Kambara pyroclastic flow/debris avalanche deposit of the asama 1783 eruption. *Proc., Inst. Nat. Sci. Nihon Univ.,* **47**, 271-286. (in Japanese with English abstract).

Tamura, C. and Hayakawa, Y. (1995) Reconstruction of the sequence of the 1783 Asama eruption from the ancient literature. *J. Geogr.* **104**, 843-864. (in Japanese with English abstract).

Tsutsumi, T. (2012) Asama: Cultural history of the foot of Asama volcano. Hoozuki shoseki publishing company, 201p. (in Japanese).

Waldhauser, F., and Ellsworth, W.L. (2000), A double difference earthquake location algorithm: method and application to the Northern Hayward Fault, California, *Bull. Seismol. Soc. Amer.,* **90**, 1353-1368.

Yasui, M., and Koyaguchi, T. (1998) Formation of a pyroclastic cone in the 1783 plinian eruptions of Asama Volcano. *Bull. Volcanol. Soc. Japan* **43**, 457-465. (in Japanese with English abstract).

Yasui, M., and Koyaguchi, T. (2004) Sequence and Eruptive Style of the 1783 Eruption of Asama Volcano, Central Japan: A case study of an andesitic explosive eruption generating fountain-fed lava flow, pumice fall, scoria flow and forming a cone. *Bull. Volcanol.,* **66**, 243-262.

Yasui, M., Koyaguchi., and T, Aramaki, S. (1997) Plinian eruptions in the 1783 activity of Asama volcano inferred from the deposits and the old records. *Bull. Volcanol. Soc. Japan* **42,** 281-297. (in Japanese with English abstract).

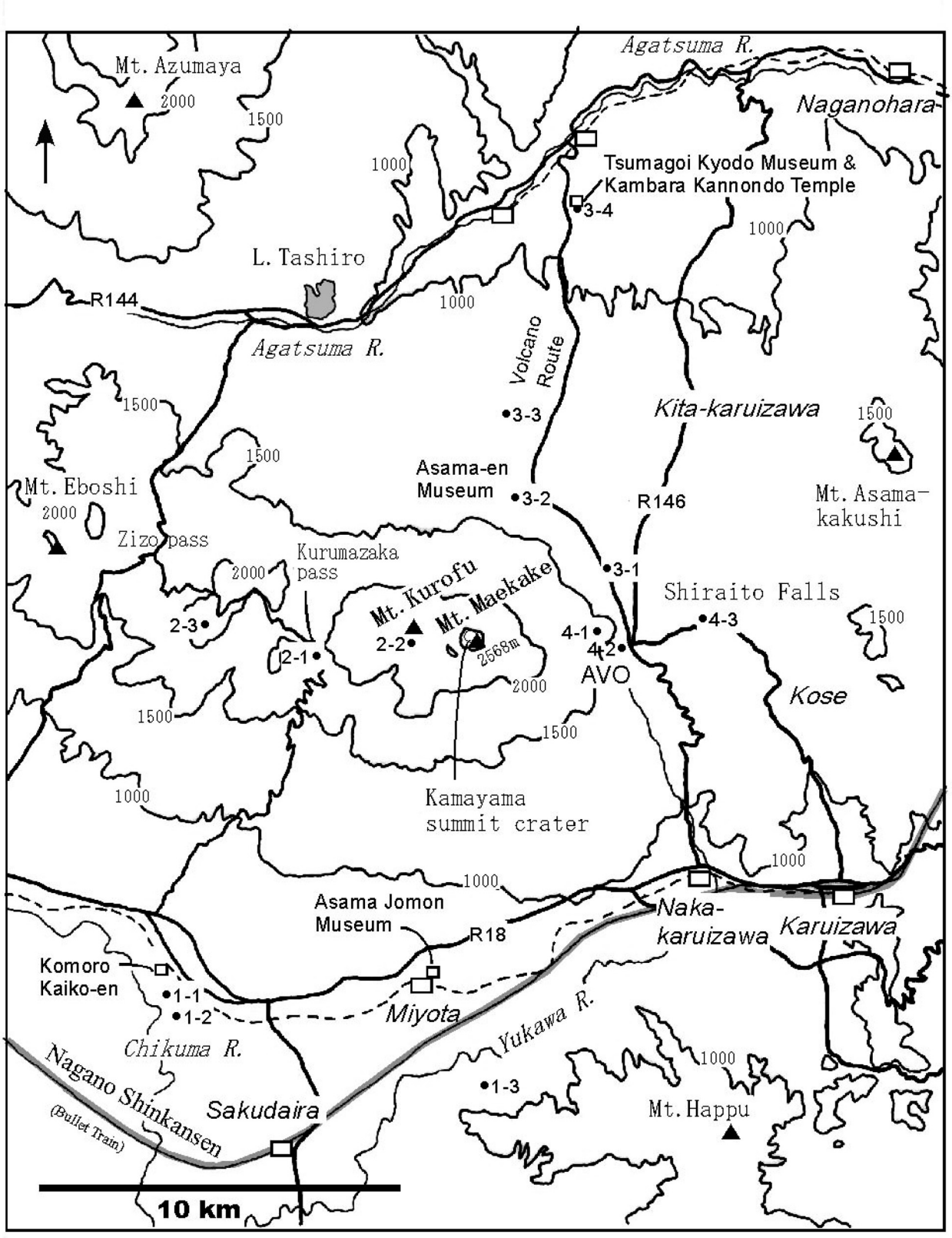

Fig. 40 Map showing the Asama-Eboshi volcano group and surrounding area. The stops in the field trip are also shown.